Magnetic heterostructures and nanoscopic materials

Denys Makarov

Dresden, Germany

Dresden (~800 years old & ~500.000 inhabitants):

Capital of the Free State of Saxony

Scientific landscape:

Technical University of Dresden: about 40.000 students

Max Planck Institutes: 3 | Leibniz Institutes: 3
Fraunhofer Institutes: 8 | Helmholtz Institute: 1

Helmholtz-Zentrum Dresden-Rossendorf (HZDR)

Research for the World of Tomorrow

Established	1992 (1955)
Member of Helmholtz Association	2011
Base Budget	~ 100 Mio. €/a
Employees	~ 1400

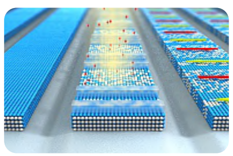

8 Institutes

10 Young Investigator Groups

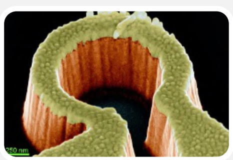

Sites: DRESDEN

Grenoble, Freiberg, Leipzig

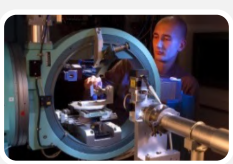

RESEARCH AREAS

ENERGY

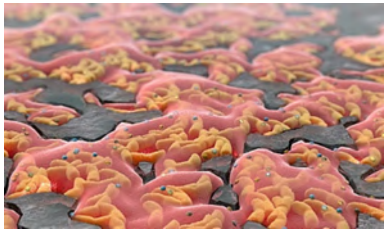

HEALTH (→ Oncology)

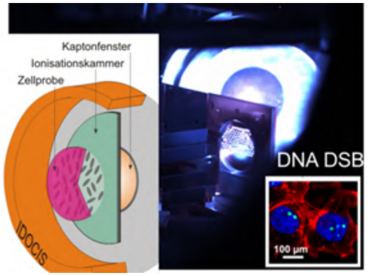

MATTER (→ Materials)

HZDR Facilities

- User Facilities

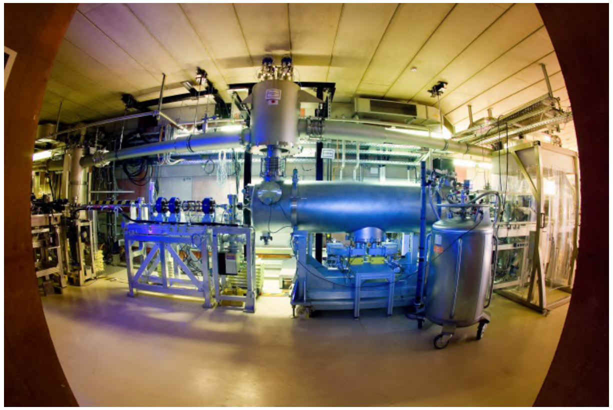

ELBE.

Center for High-Power Radiation Sources

IBC.

Ion Beam Center

Industry Services via

HZDR INNOVATION

HLD.

High-Magnetic Field Laboratory

PET Center

DRESDEN concept HZDR

Overview of activities

I. Curvilinear magnetism (3-dimentional geometries)

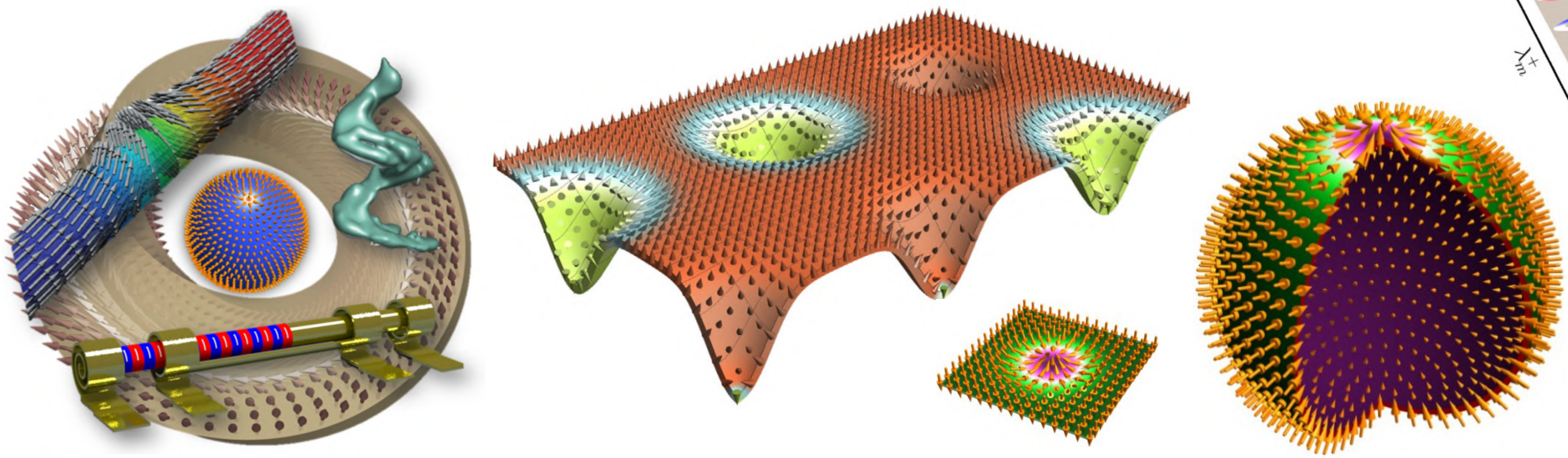

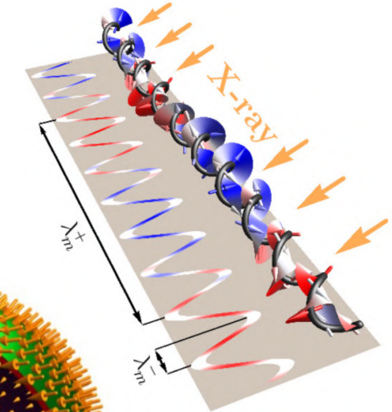

Nature Physics & Nature Communications & Phys. Rev. Lett. & Nano Letters & Advanced Materials & Appl. Phys. Lett.

II. Flexible sensors & actuators

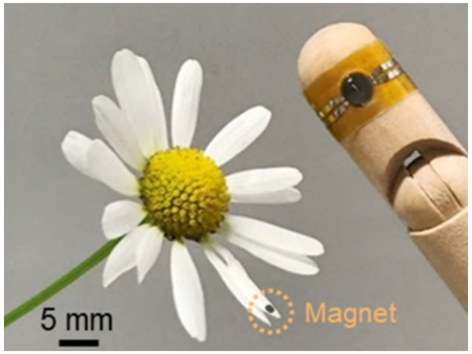

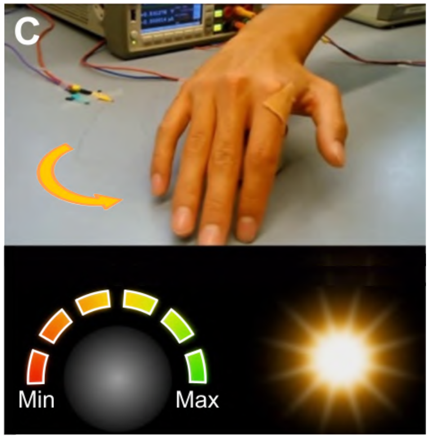

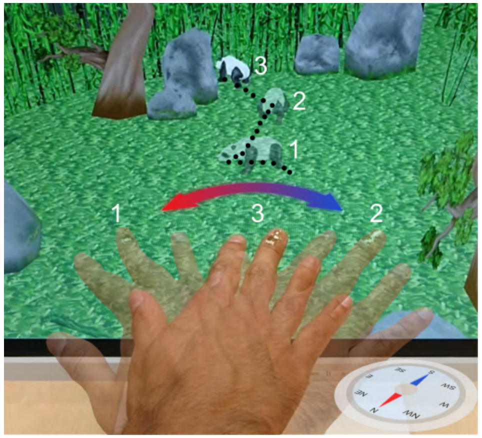

Science Advances & Nature Electronics & Nano Letters & Advanced Materials & Adv. Funct. Mater. & Nature Commun.

Review: Santiago Canon and DM, *Adv. Funct. Mater.* (2021). doi:10.1002/adfm.202007788

DRESDEN concept HZDR

Definition

Nanoscopic materials

Impact of reduced dimensionality on the material properties

Multidomain vs Single domain state

Ferromagnetism vs Superparamagnetism

What is the origin of the observed differences in magnetic behavior between a sample with nanometric dimensions and a macroscopic sample of the same material? These differences are shown to arise from broken translation symmetry in nanometric samples, from the higher proportion of atoms on the surface, or interface, from the fact that the sizes of objects of nanoscopic scale, or nanoscale are comparable to some fundamental or characteristic lengths of the constituent material and other effects. The exchange length and the magnetic domain wall width are some of the characteristic lengths that are more relevant to the magnetic properties.

Alberto P. Guimarães, Principles of Nanomagnetism, Springer (2017)

Definition

Nanoscopic materials

Impact of reduced dimensionality on the material properties

Multidomain vs Single domain state

Ferromagnetism vs Superparamagnetism

Impact of the geometry of the object

Micromagnetism

(minimalistic)

1. A. Aharoni: *Introduction to the theory of ferromagnetism* (1996)
2. R.C. O'Handley: *Modern magnetic materials: Principles and applications* (2000)

Dr. Denys Makarov I E-Mail: d.makarov@hzdr.de I Intelligent Materials and Systems

Formation of magnetic domains

In 1907, Weiss proposed the concept of magnetic domains. Those are regions inside the material that are magnetized in different direction. Domain walls separate domains.

P. Weiss, J. Phys. 6 (1907) 401.

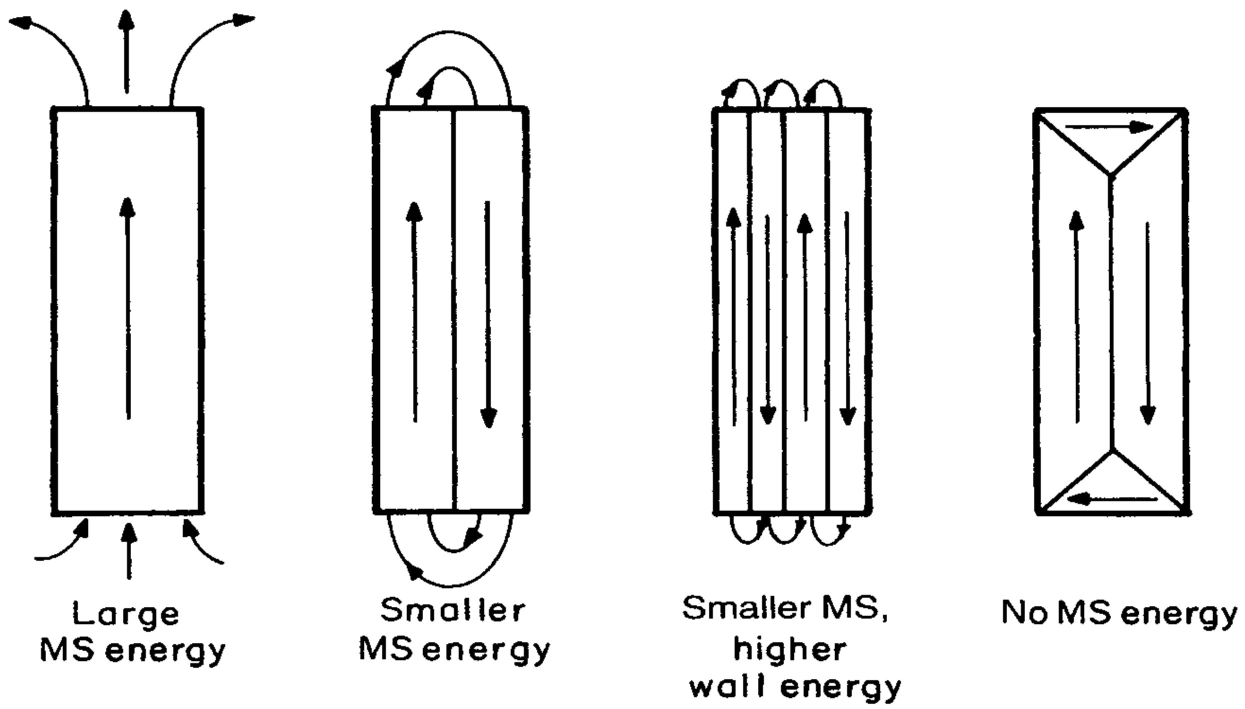

Domain formation results in the minimisation of the magnetostatic (MS) energy. Introduction of 180deg domain walls reduces the MS energy but increases the domain wall energy; 90deg closure domains eliminate MS energy but increase anisotropy energy in uniaxial materials.

Relevant energy densities

Exchange energy

$$f_{\text{ex}} = -\frac{2JS^2}{a^3}\cos\theta_{ij} = A\left(\frac{\partial\theta}{\partial x}\right)^2 \xrightarrow{3D} A\sum_{i=1}^{3}\left(\frac{\nabla M_i}{M_S}\right)^2$$

Magnetostatic

$$f_{ms} = -\mu_0 M_S \cdot H_i = \frac{\mu_0}{2} M_S^2 \cos^2\theta$$

Magnetocrystalline

$$f_a = K_2 \sin^2\theta + K_4 \sin^4\theta + \cdots \text{(uniaxial)}$$

$$f_a = K_1(\alpha_1^2\alpha_2^2 + \alpha_2^2\alpha_3^2 + \alpha_3^2\alpha_1^2) + K_2\alpha_1^2\alpha_2^2\alpha_3^2 + \cdots \text{(cubic)}$$

Magnetoelastic

$$f_{me}^{\text{iso}} \approx B_1 e_{33} \sin^2\theta = \lambda_S^2 E \cos^2\theta = \tfrac{3}{2}\lambda_S \sigma \cos^2\theta$$

Zeeman

$$f_{\text{Zeeman}} = -M \cdot B$$

Minimization of the sum of these energy densities results in equilibrium magnetic state of the sample

Dr. Denys Makarov I E-Mail: d.makarov@hzdr.de I Intelligent Materials and Systems

Domain walls

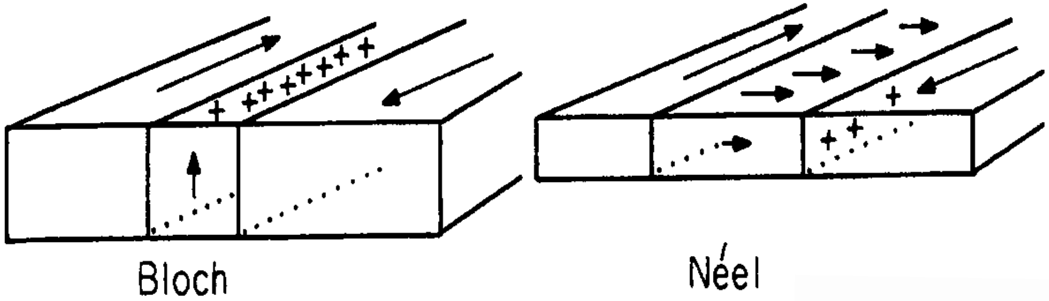

Bloch wall: charged surface on the external surface of the sample

Neel wall: charged surface internal to the sample

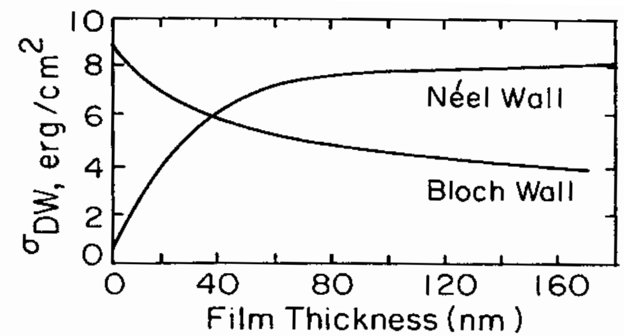

Domain wall energy density (per area):

$$\sigma_{dw} = 4(AK)^{1/2}$$

Domain wall width parameter = $(A/K)^{1/2}$

Energy per unit area and width of Bloch and Néel wall as function of the film thickness

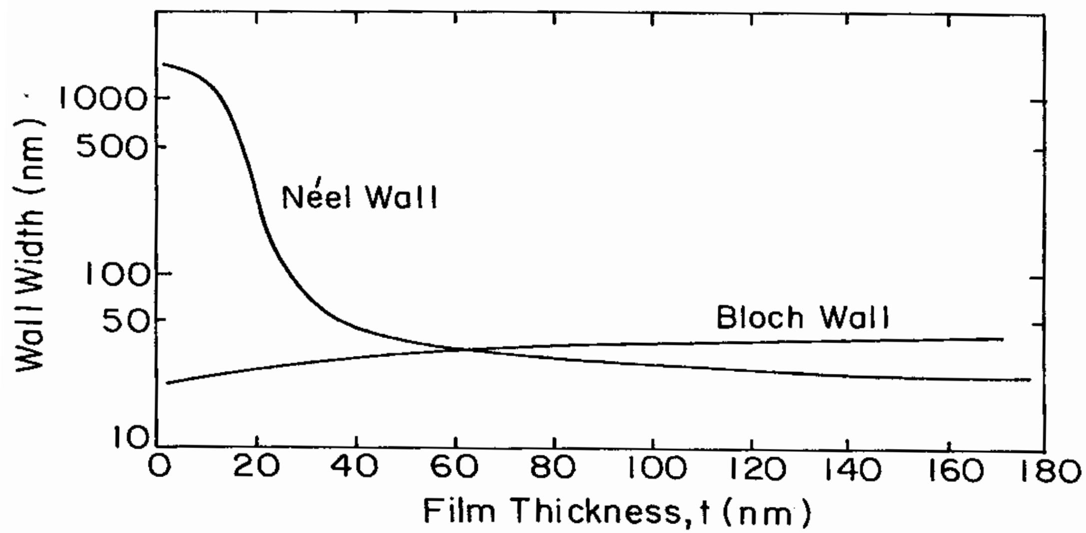

Parameters for calculation:

$A = 10^{-11}$ J/m

$M_s = 1$ T

$K = 100$ J/m^3

Concept of single domain particles:
Magnetic data storage

Patterned magnetic media

$L1_0$ chemically ordered FePt alloy allows thermal stability for 3-nm-large grains

Single grain ⇔ Single bit => Patterned Magnetic Media

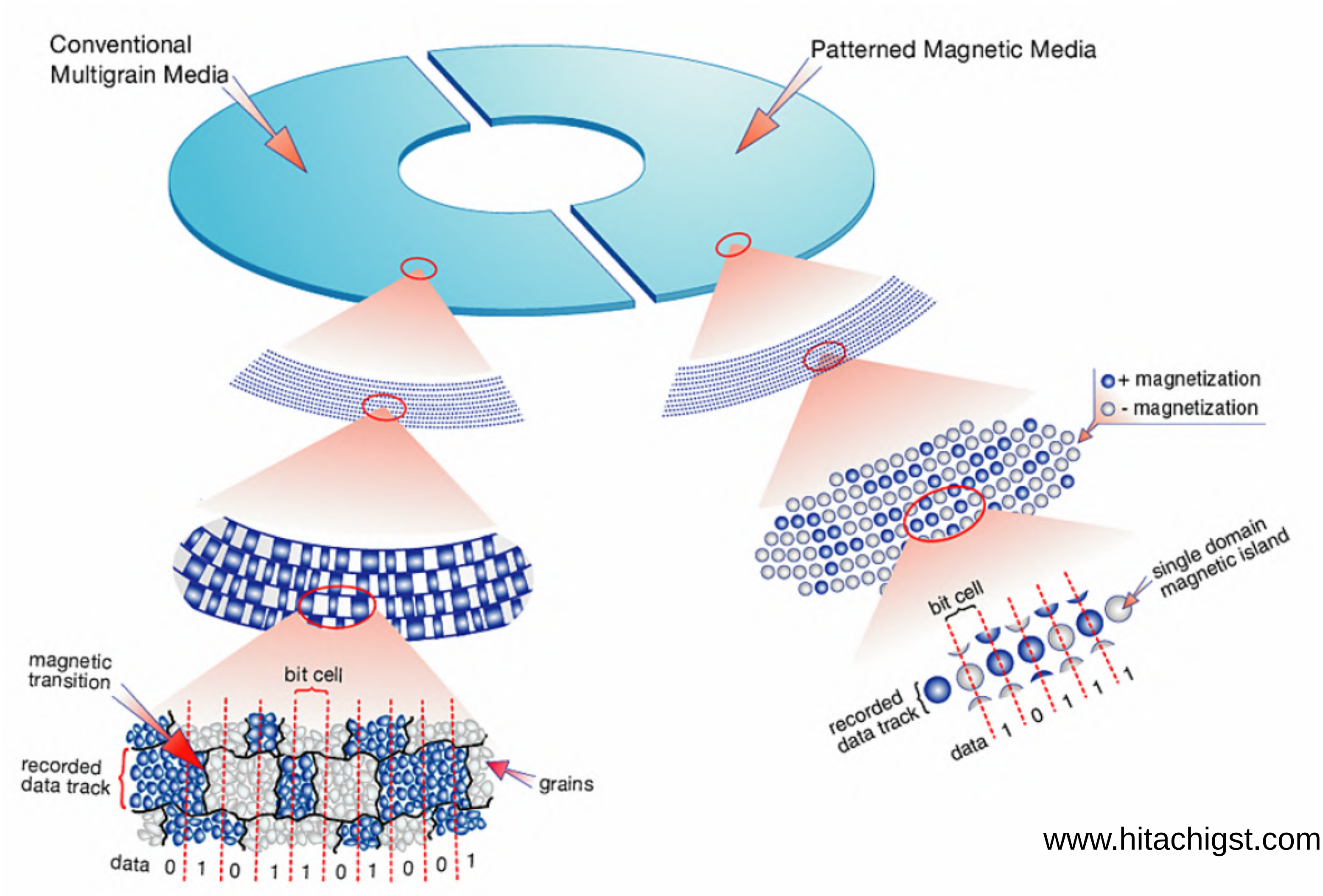

www.hitachigst.com

Single domain particles

The critical radius of a spherically shaped particle is defined when the energy of a domain wall spanning a spherical particle is equal the change of the magnetostatic energy for a single- and two-domain states

$$\sigma_{dw} S = 4\pi r^2 (AK)^{1/2} \quad \text{vs.} \quad \triangle E_{MS} \approx 1/2 \times 1/3\ (1- a_0)\ u_o\ M_s^2\ V$$

$a_0 \approx 0.5$

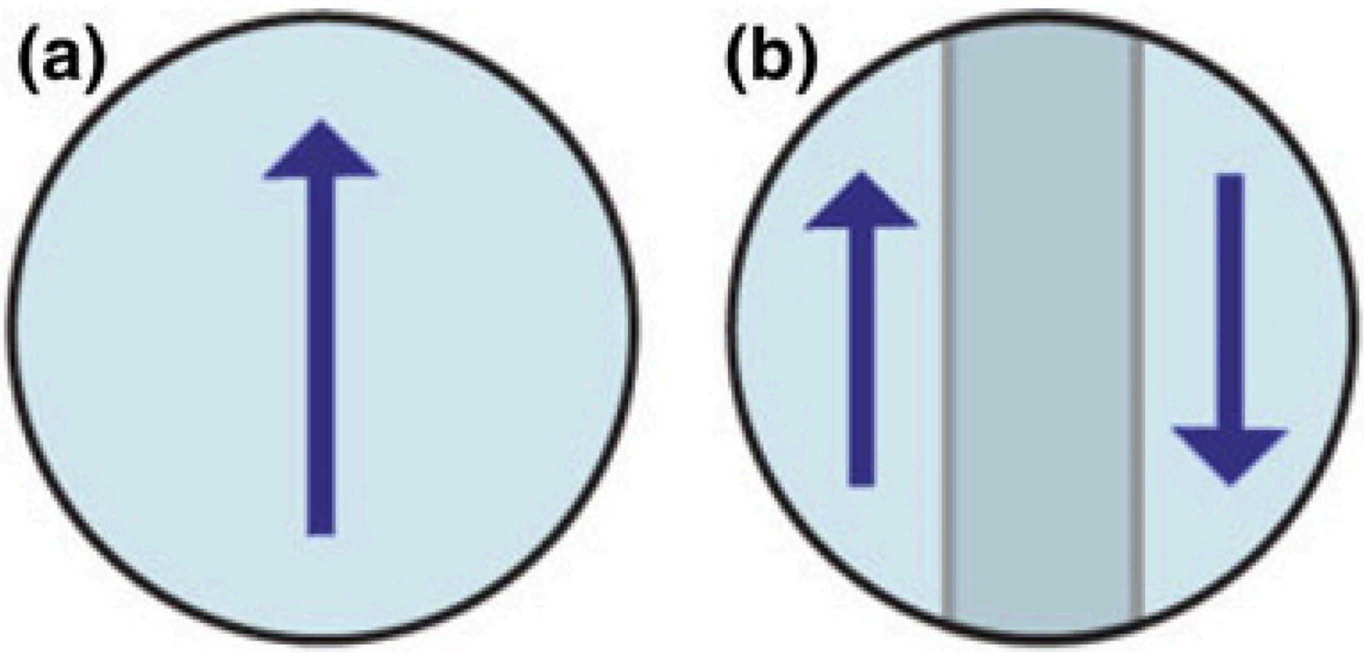

Alberto P. Guimarães, Principles of Nanomagnetism, Springer (2017)

Single domain particles

The critical radius of a spherically shaped particle is defined when the energy of a domain wall spanning a spherical particle is equal the change of the magnetostatic energy for a single- and two-domain states

$\sigma_{dw}\, S = 4\pi r^2 (AK)^{1/2}$ vs. $\triangle E_{MS} \approx 1/2 \times 1/3\, (1- a_0)\, u_o\, M_s^2\, V$

$a_0 \approx 0.5$

$$r_c \approx 36 \frac{(AK_u)^{1/2}}{\mu_0 M_s^2} \quad (\text{large } K_u)$$

$r_c \approx$ 3 nm for Fe

$r_c \approx$ 30 nm for γFe_2O_3

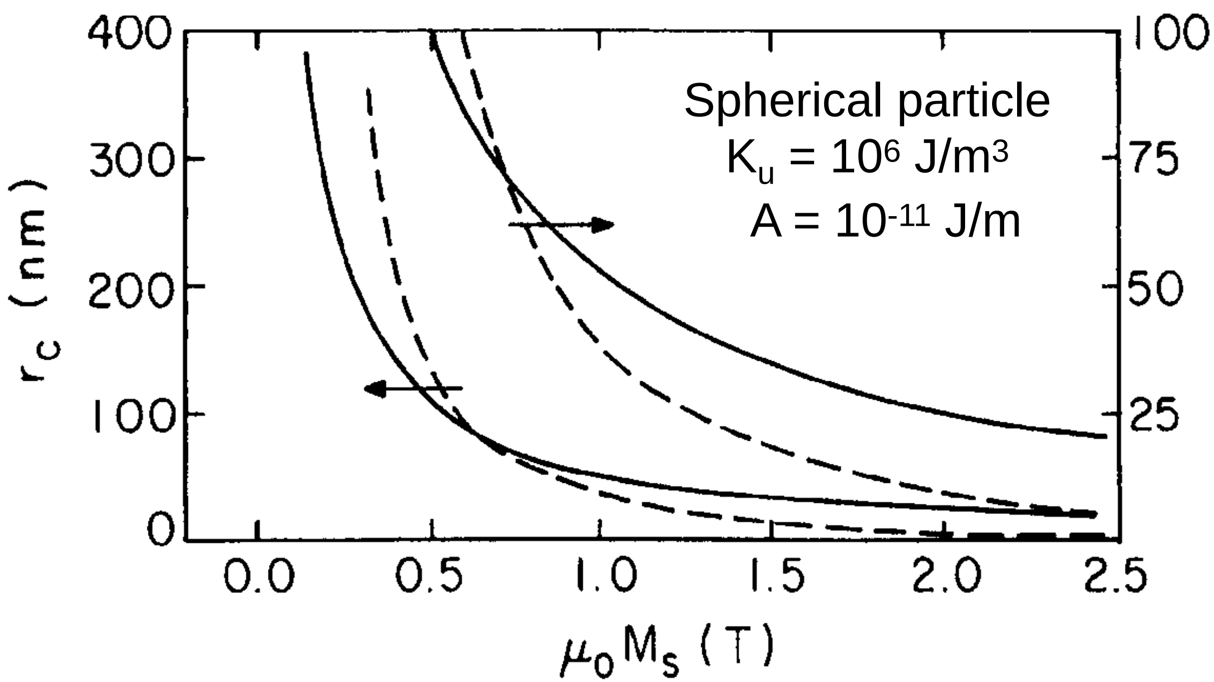

Information bits in perpendicular recording media

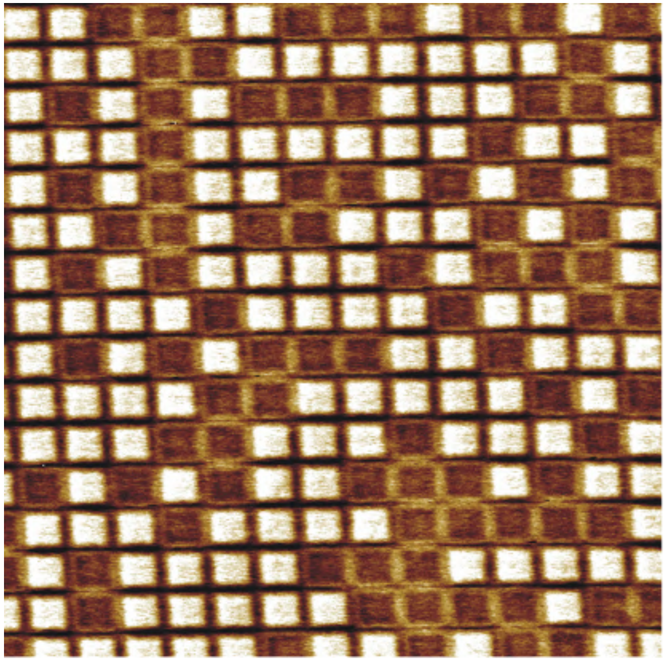

Higher areal density <=> Reduce the bit size

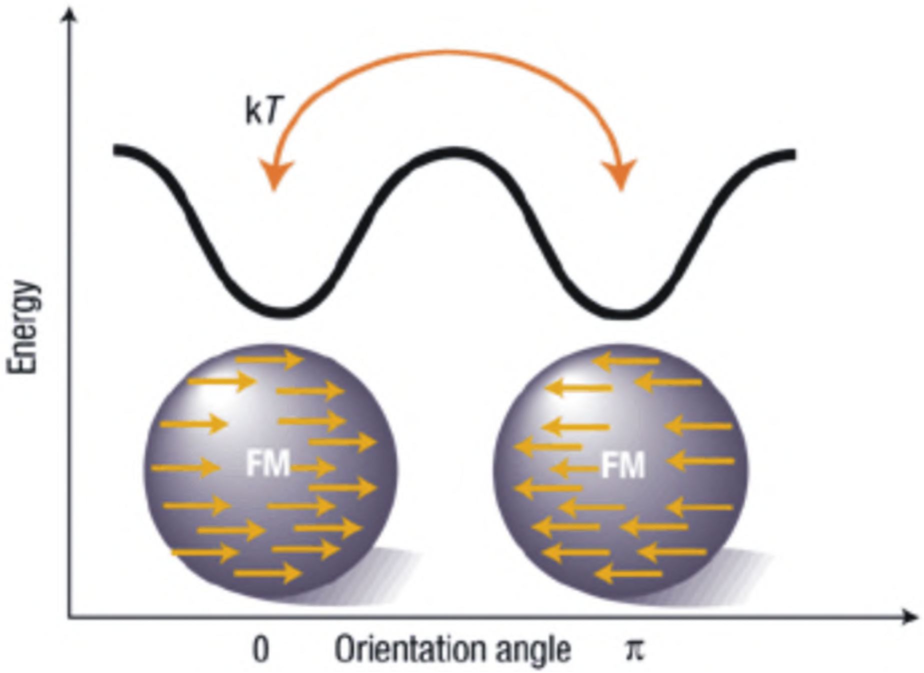

Bit size: 50 nm

A: 10^{-11} J/m

M_S: 0.6 T

K_U: 1 MJ/m^3

Criteria: Long time stability (~10 years)

[Anisotropy Energy] = 60 x [Thermal Energy]

$$K_U \cdot V = 60 \cdot k_B \cdot T$$

Piramanayagam, *J. Appl. Phys.* **102** (2007) 011301

Eisenmenger et al., *Nature Mater.* **2** (2003) 437

Superparamagnetism

Paramagnetism describes the tendency of a material to be attracted to a permanent magnet due to the presence of least one unpaired electron in a material

Superparamagnetism: deals with small particle, which are ferromagnetic. At long time scale (measurement time is longer than the relaxation time) the particle behaves as paramagnet. Application of an external magnetic field results in a much stronger magnetic response than would be the case for a paramagnet

Probability P per unit time for switching of a nanoparticle:

$$P = \nu_0 \exp\left(-\frac{\Delta f V}{k_B T}\right)$$

the first term in the right side is an attempt frequency factor equal approximately 10^9 s^{-1}. Δf is equal to the anisotropy constant.

For a spherical particle with $K_u = 10^5$ J/m^3 the superparamagnetic radii for stability over 1 year and 1 second, respectively:

$$r_0^{1\,\mathrm{yr}} \approx \left(\frac{10 k_B T}{K_u}\right)^{1/3} \approx 7.3\ \mathrm{nm}, \qquad r_0^{1\,\mathrm{s}} \approx \left(\frac{6 k_B T}{K_u}\right)^{1/3} \approx 6\ \mathrm{nm}$$

Dr. Denys Makarov I E-Mail: d.makarov@hzdr.de I Intelligent Materials and Systems

Effect of geometrical curvature

3D curved magnetic shell structures

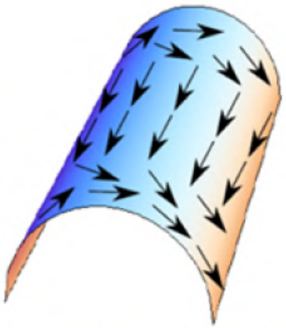

Cylindrical surfaces

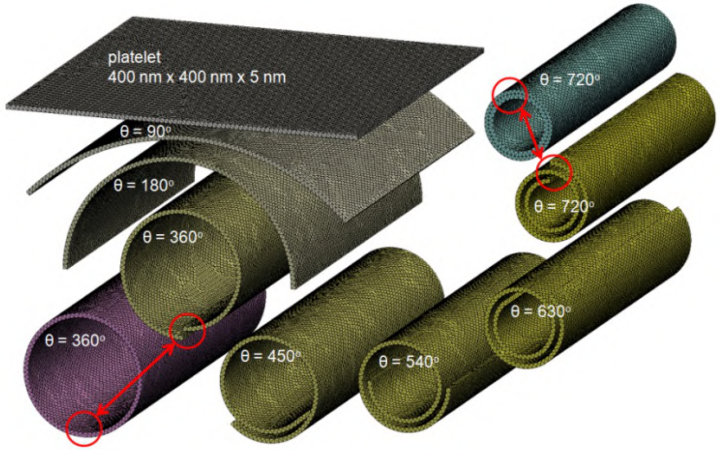

Streubel et al., *Nano Lett.* (2012) & (2014) & *Adv. Mat.* (2014)

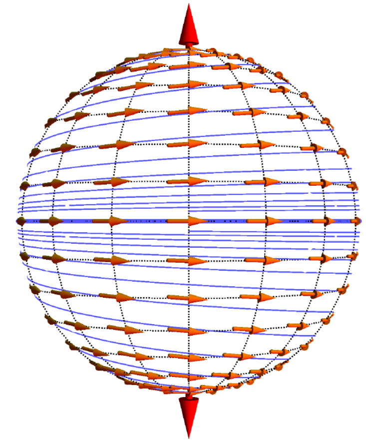

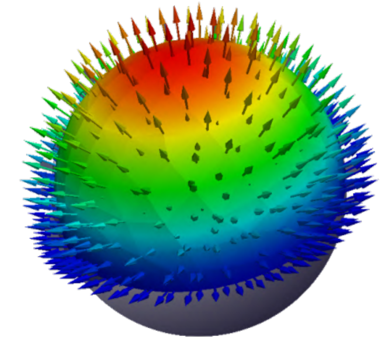

Spherical surfaces

Albrecht et al., *Nat. Mater.* **4**, 203 (2005)
Ulbrich et al., *PRL* (2006); DM et al., *APL* (2007)…
Kravchuk et al., *PRB* **85**, 144433 (2012)

Curvature induced skyrmions on a sphere

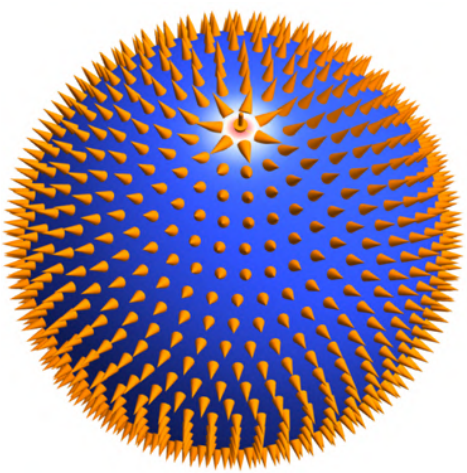

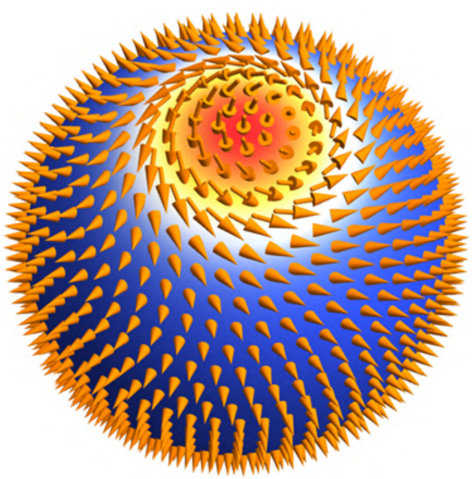

Kravchuk et al., *PRB* (2016); *PRL* (2018)

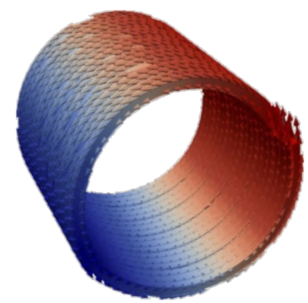

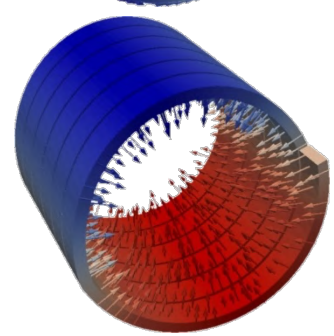

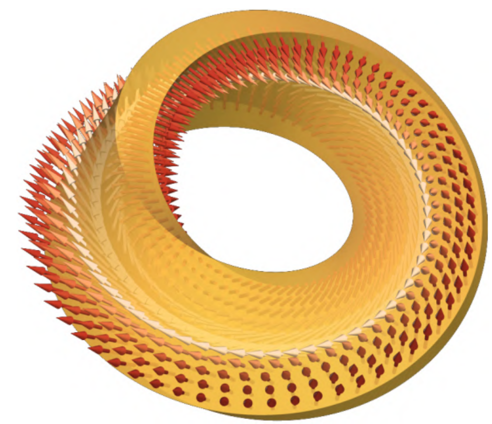

Pylypovskyi et al., *PRL* ('15)

Smith et al.,
PRL **107**, 097204 (2011)

DRESDEN concept HZDR

Experimental realizations

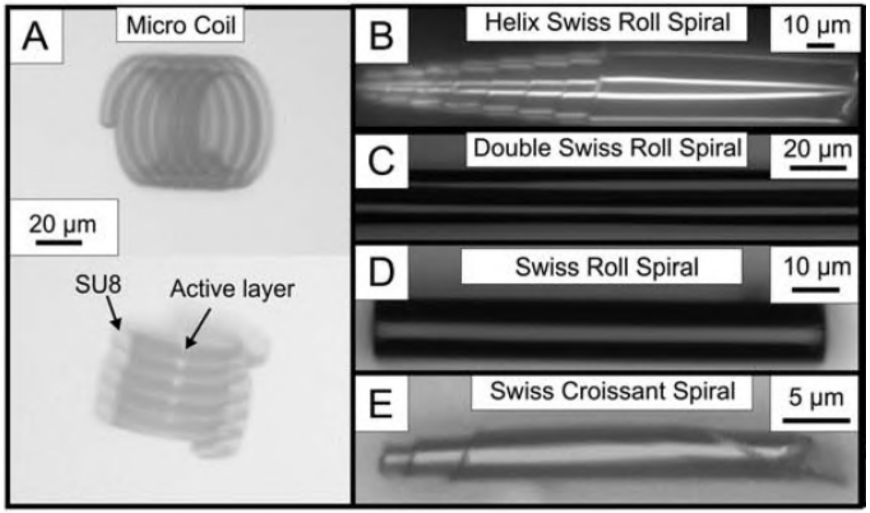

Smith et al., *Phys. Rev. Lett.* (2011) & *Soft Mat.* (2011)

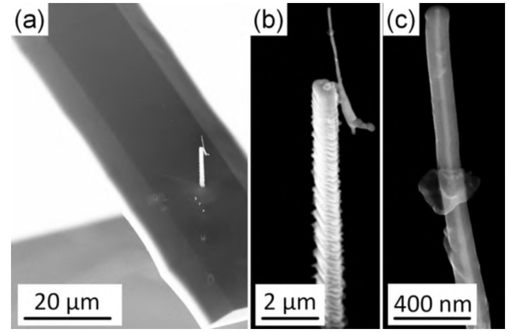

Mühl et al., *APL* (2012)

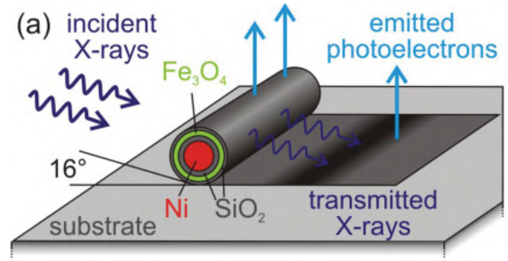

Kimling et al., *PRB* (2011)

Magnetic soft x-ray tomography

Streubel et al., *Nature Commun.* (2015)

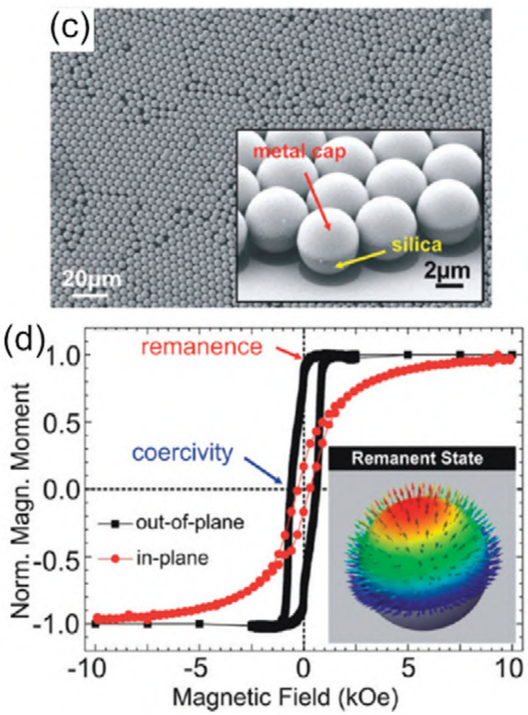

Baraban et al., *ACS Nano* (2012)

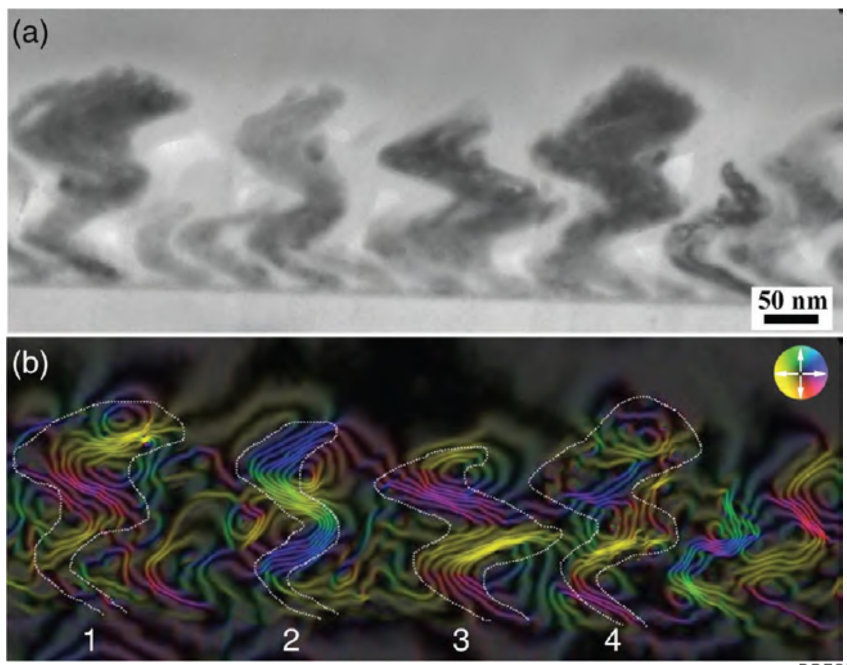

Phatak et al., *Nano Lett.* (2014)

Impact of curvature on a magnetic system

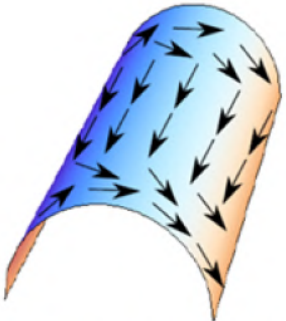

Cylindrical surfaces

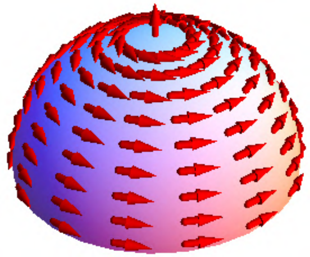

Spherical surfaces

Magnetic interactions in the anisotropic Heisenberg ferromagnet:

$$E = L \int_{\mathcal{S}} \left[A \sum_{i=x,y,z} (\nabla m_i)^2 + K(\boldsymbol{m}\cdot\boldsymbol{n})^2 \right] \mathrm{d}\mathcal{S}$$

Exchange energy   Anisotropy energy

In a curvilinear basis, micromagnetic energy can be rewritten:

$$\mathscr{E}_{ex} = [\boldsymbol{\nabla}\theta - \boldsymbol{\Gamma}(\varphi)]^2 + \left[\sin\theta\,(\boldsymbol{\nabla}\varphi - \boldsymbol{\Omega}) - \cos\theta \frac{\partial\boldsymbol{\Gamma}(\varphi)}{\partial\varphi}\right]^2$$

$$\mathscr{E}_{ex} = \mathscr{E}_{ex}^{0} + \mathscr{E}_{ex}^{A} + \mathscr{E}_{ex}^{D} \qquad \mathscr{E}_{ex}^{0} = (\boldsymbol{\nabla}\theta)^2 + \sin^2\theta(\boldsymbol{\nabla}\varphi)^2$$

Induced anisotropy responses:

$$\mathscr{E}_{ex}^{A} = \boldsymbol{\Gamma}^2 + \sin^2\theta\boldsymbol{\Omega}^2 + \cos^2\theta(\partial_\varphi\boldsymbol{\Gamma})^2$$

Quadratic in curvature

Induced chiral responses:

$$\mathscr{E}_{ex}^{D} = D_{\alpha\beta\gamma} m_\beta \nabla_\gamma m_\alpha, \quad D_{\alpha\beta\gamma} = -D_{\beta\alpha\gamma}$$

$$\mathscr{E}_{ex}^{D} = -2\left[(\boldsymbol{\nabla}\theta\cdot\boldsymbol{\Gamma}) + \sin\theta\boldsymbol{\nabla}\varphi\cdot(\boldsymbol{\Omega} + \cos\theta\partial_\varphi\boldsymbol{\Gamma})\right]$$

Linear in curvature

Gaididei et al., *PRL* (‘14); Pylypovskyi, DM et al., *PRL* (‘15); Kravchuk, DM et al., *PRL* (‘18); Volkov, DM et al., *PRL* (‘19)…

Impact of curvature on a magnetic system

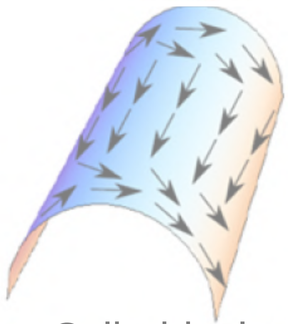

Cylindrical surfaces

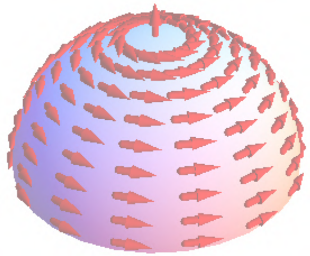

Spherical surfaces

Magnetic interactions in the anisotropic Heisenberg ferromagnet:

$$E = L\int_{\mathcal{S}}\left[A\sum_{i=x,y,z}(\nabla m_i)^2 + K(\boldsymbol{m}\cdot\boldsymbol{n})^2\right]\mathrm{d}\mathcal{S}$$

Exchange energy Anisotropy energy

New approach to material science

designing magnetic responses by tailoring the geometry of thin films

Induced anisotropy responses: $\mathscr{E}_{ex}^{A} = \boldsymbol{\Gamma}^2 + \sin^2\theta\boldsymbol{\Omega}^2 + \cos^2\theta(\partial_\varphi\boldsymbol{\Gamma})^2$ Quadratic in curvature

Induced chiral responses: $\mathscr{E}_{ex}^{D} = D_{\alpha\beta\gamma}m_\beta\nabla_\gamma m_\alpha, \quad D_{\alpha\beta\gamma} = -D_{\beta\alpha\gamma}$

$\mathscr{E}_{ex}^{D} = -2\left[(\boldsymbol{\nabla}\theta\cdot\boldsymbol{\Gamma}) + \sin\theta\boldsymbol{\nabla}\varphi\cdot(\boldsymbol{\Omega} + \cos\theta\partial_\varphi\boldsymbol{\Gamma})\right]$ Linear in curvature

Gaididei et al., *PRL* (‘14); Pylypovskyi, DM et al., *PRL* (‘15); Kravchuk, DM et al., *PRL* (‘18); Volkov, DM et al., *PRL* (‘19)…

Experimental confirmation of curvature effects

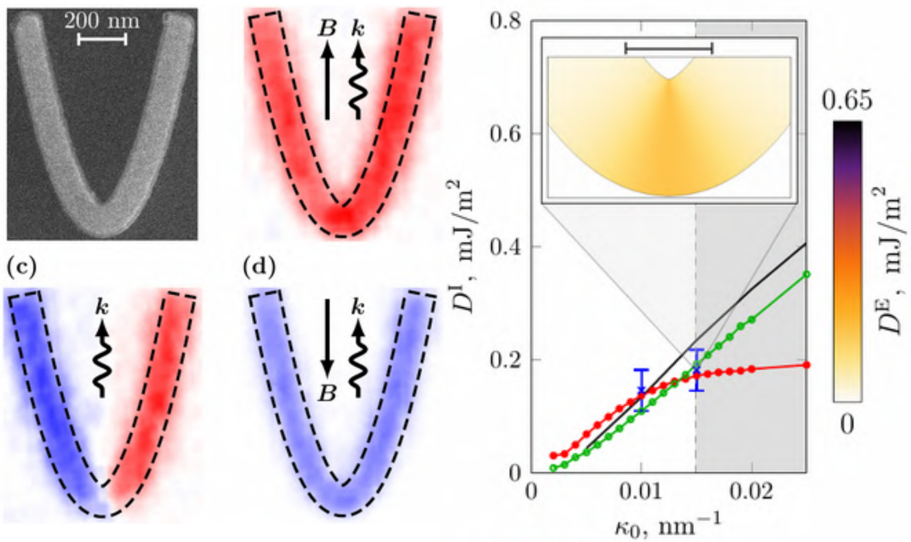

Volkov et al., *Phys. Rev. Lett.* **123**, 077201 (2019)

Magnetic Skyrmion states on a curvilinear defect

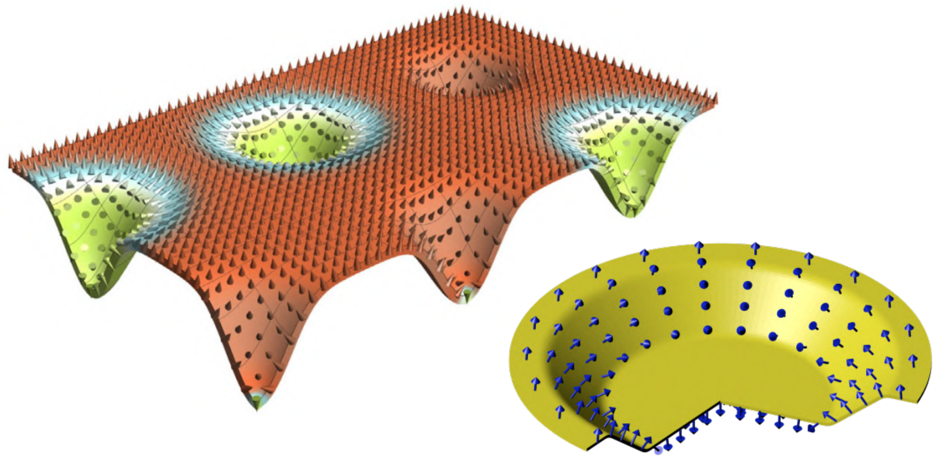

Kravchuk et al., *Phys. Rev. Lett.* **120**, 067201 (2018)

Pylypovskyi et al., *Phys. Rev. Appl.* **10**, 064057 (2018)

Discovery of a non-local chiral effect in curvilinear ferromagnetic shells

Micromagnetism of *flat* thin films

Micromagnetism in *curved* geometries

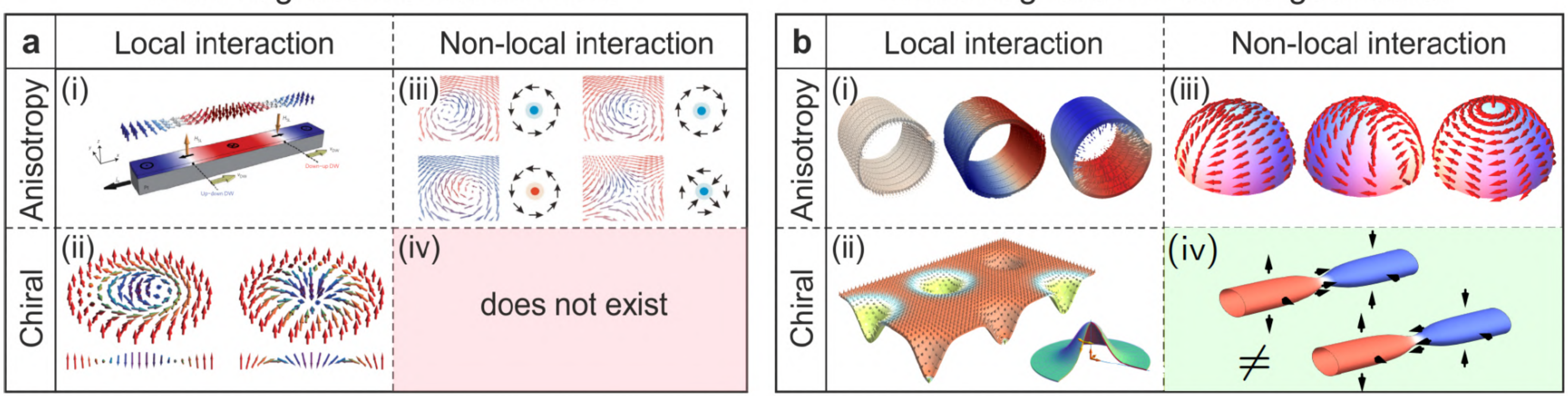

Sheka et al., *Communications Physics* **3**, 128 (2020)

Magnetic heterostructures

Definition

Heterostructures

Heterostructures show different synergistic relations between two or more building blocks that improve functional characteristics

Each component plays a complementary role in producing multifunctionality

Heterostructures consist of combinations of different materials, which are in contact through at least one interface

Magnetic heterostructures combine different physical properties which do not exist in nature

Editors: Hartmut Zabel and Samuel D. Bader
Magnetic Heterostructures: Advances and Perspectives in Spinstructures and Spintransport
Springer Trends in Modern Physics (2008)

Heterostructures

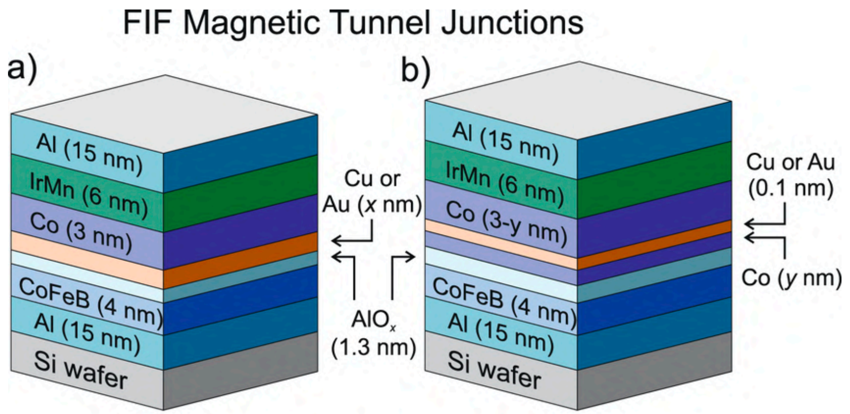

New J. Phys. 16, 043008 (2014)

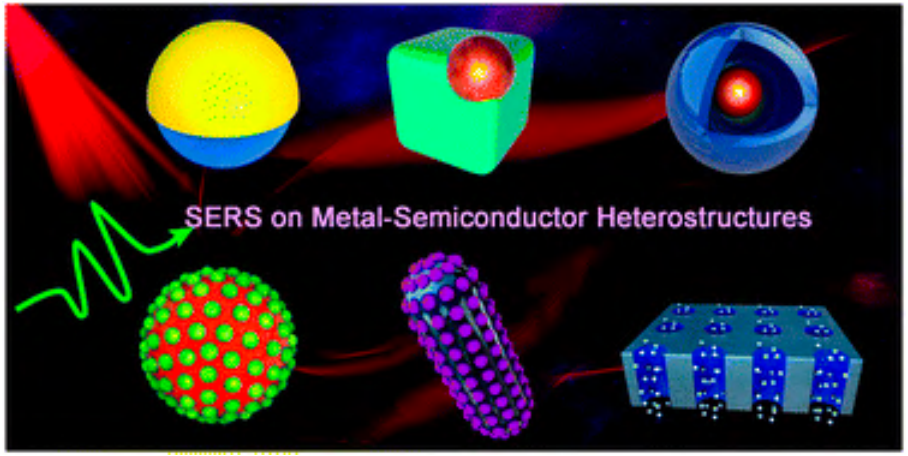

https://pubs.rsc.org/en/content/articlelanding/2021/mh/d0mh01356k

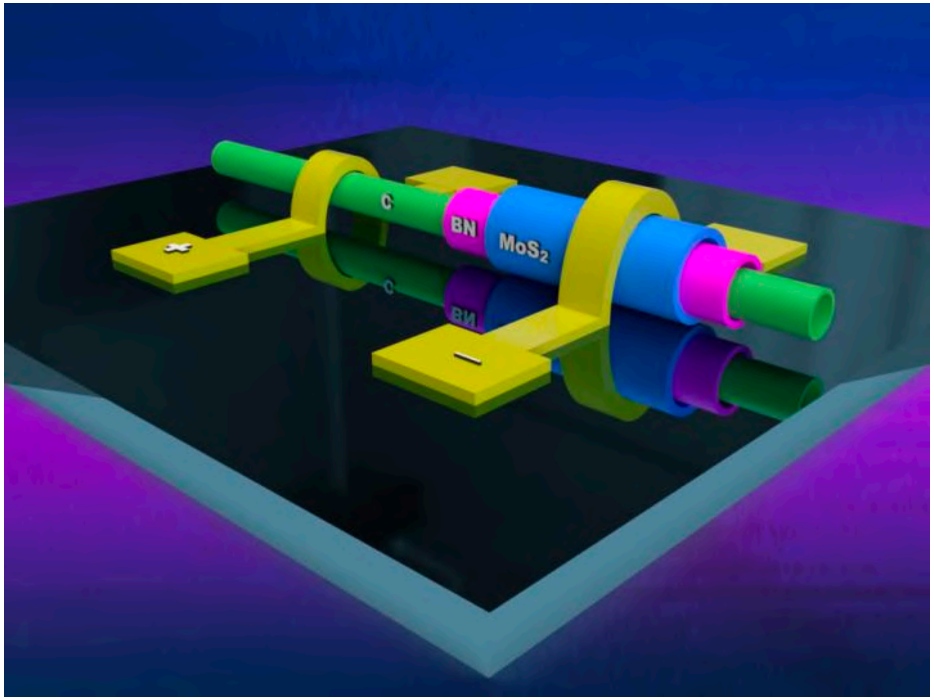

https://www.eurekalert.org/news-releases/776488

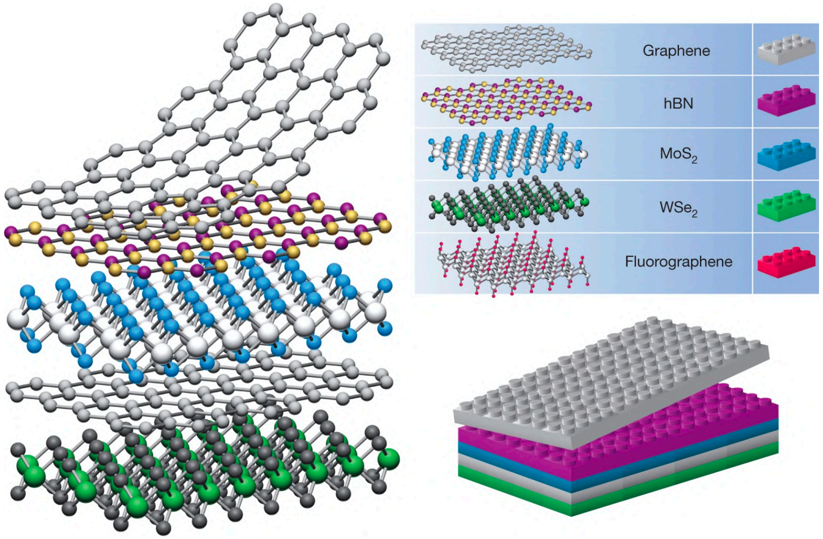

https://www.nature.com/articles/nature12385

Heterostructures of ferro- and antiferromagnets
Exchange bias effect

Magnetic sensors based on magnetoresistive effect

Read heads in magnetic data storage

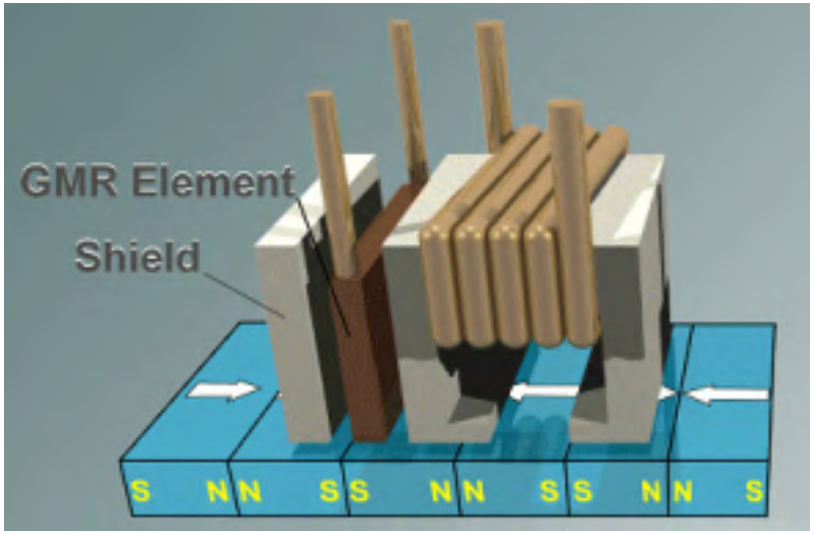

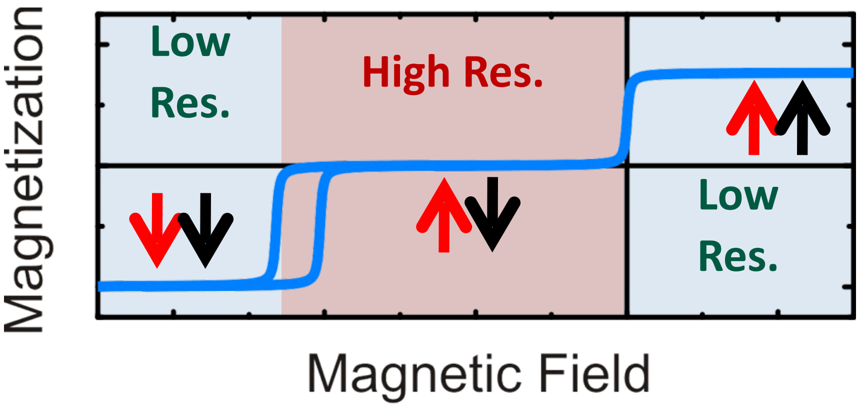

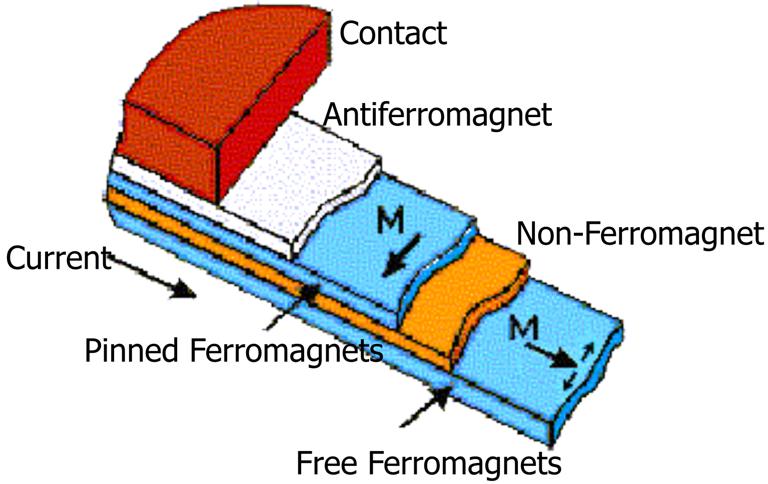

GMR sensor elements:

- Resistance change in small external fields
- Antiparallel orientation of the magnetic moment increases resistance
- Sensing layer is a soft F layer
- Reference layer pinned by exchange bias

S. S. P. Parkin, Annu. Rev. Mater. Sci. **25** (1995) 357

Exchange bias effect: coupling between F and AF layers

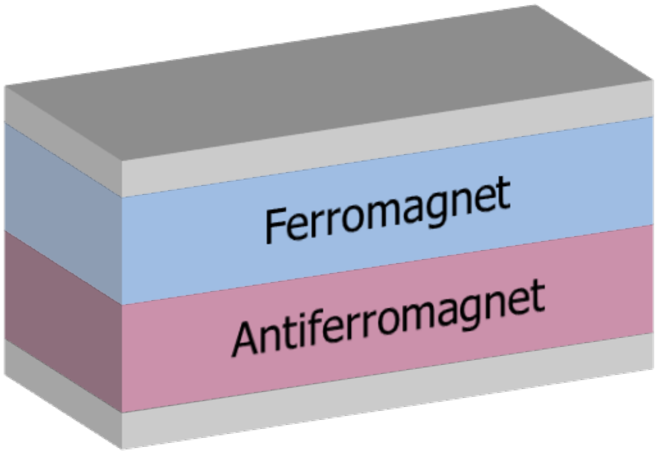

Characteristic features:

A. AF layer has to be cooled in a magnetic field

B. Hysteresis loop is shifted and broadened

C. Asymmetric magnetization reversal processes

D. Effect is strongly temperature dependent

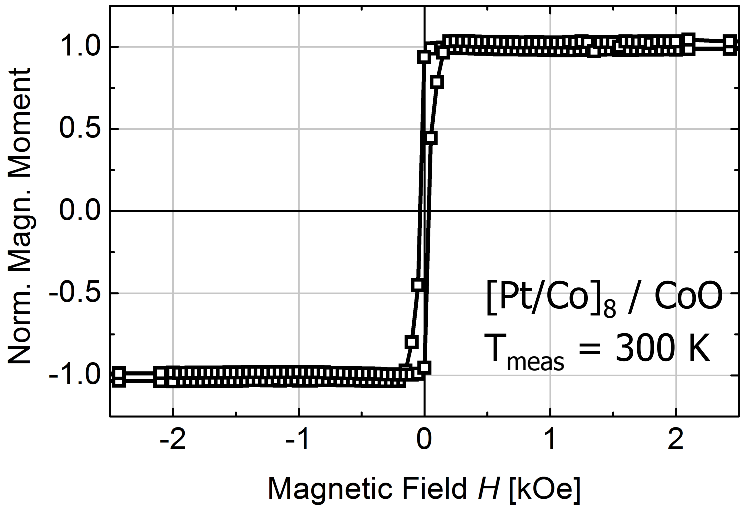

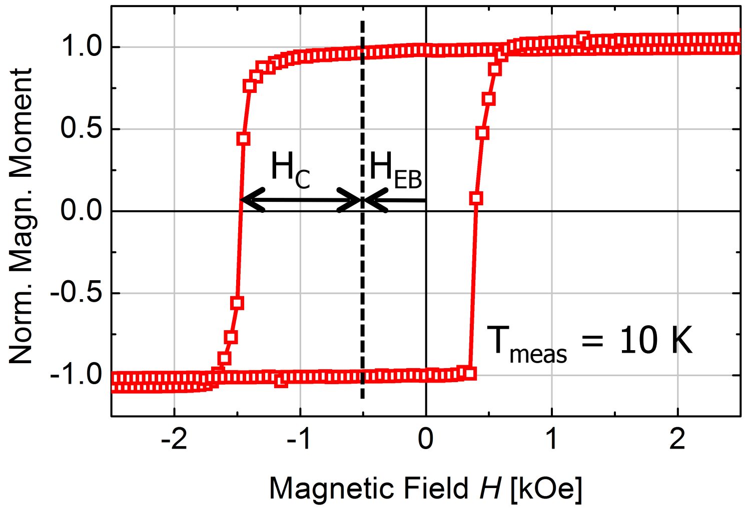

A. E. Berkowitz and K. Takano, J. Magn. Magn. Mater. **200** (1999) 552

B. K. O'Grady et al., J. Magn. Magn. Mater. **322** (2010) 883

Integral magnetic investigations of EB effect

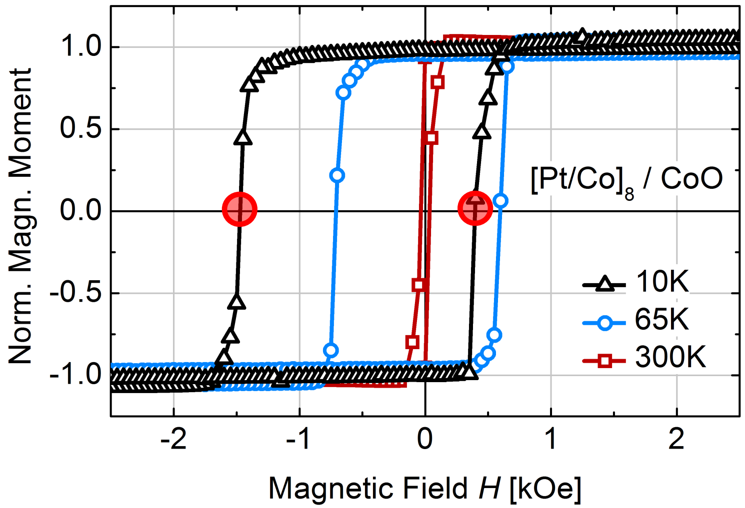

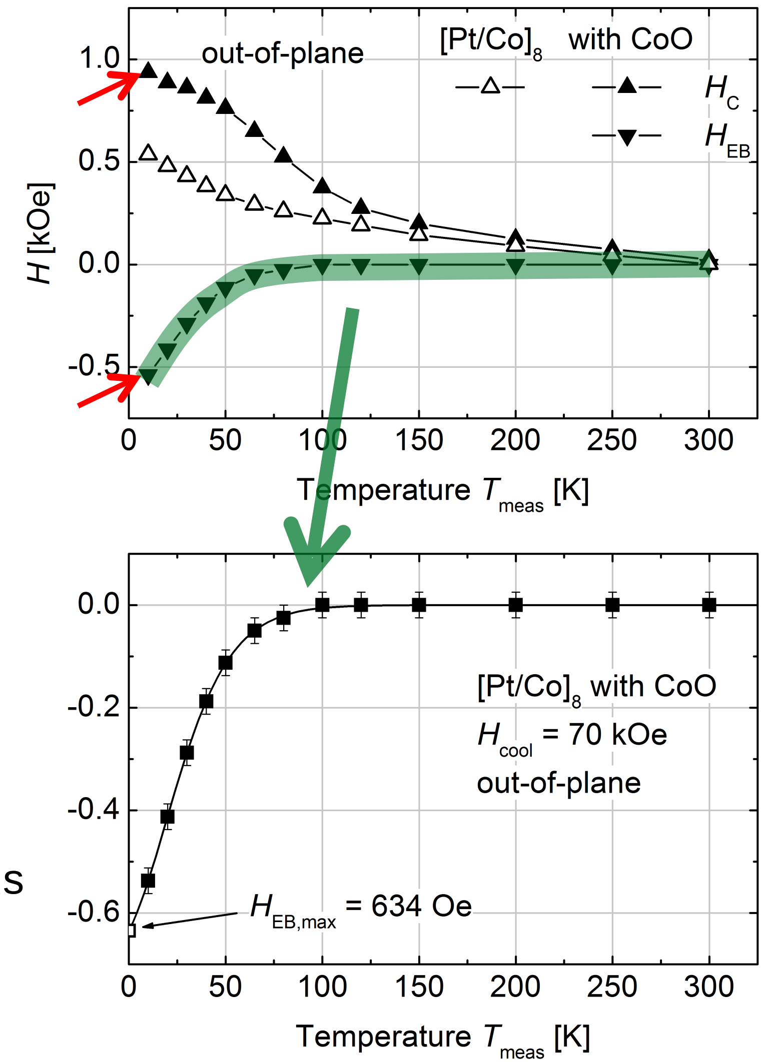

Exchange bias measurements:

(1) Warm sample to 320 K and apply H_{cool} = 70 kOe

(2) Cool sample to the measurement temperature

(3) Measure hysteresis loop and acquire coercive fields

$$H_C = (H_C^R - H_C^L) / 2 \qquad H_{EB} = (H_C^R + H_C^L) / 2$$

K. O'Grady et al., J. Magn. Magn. Mater. **322** (2010) 883
M. D. Stiles and R. D. McMichael, Phys. Rev. B **63** (2001) 064405

IrMn/$(Co/Pt)_4$ exchange bias system

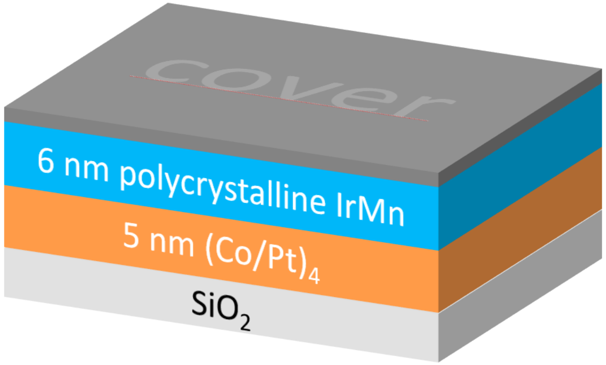

Probe coupling at nm scales

Distinct behaviour of bulk and interface in 6 nm IrMn

Field-cooled from 45°C to 7°C

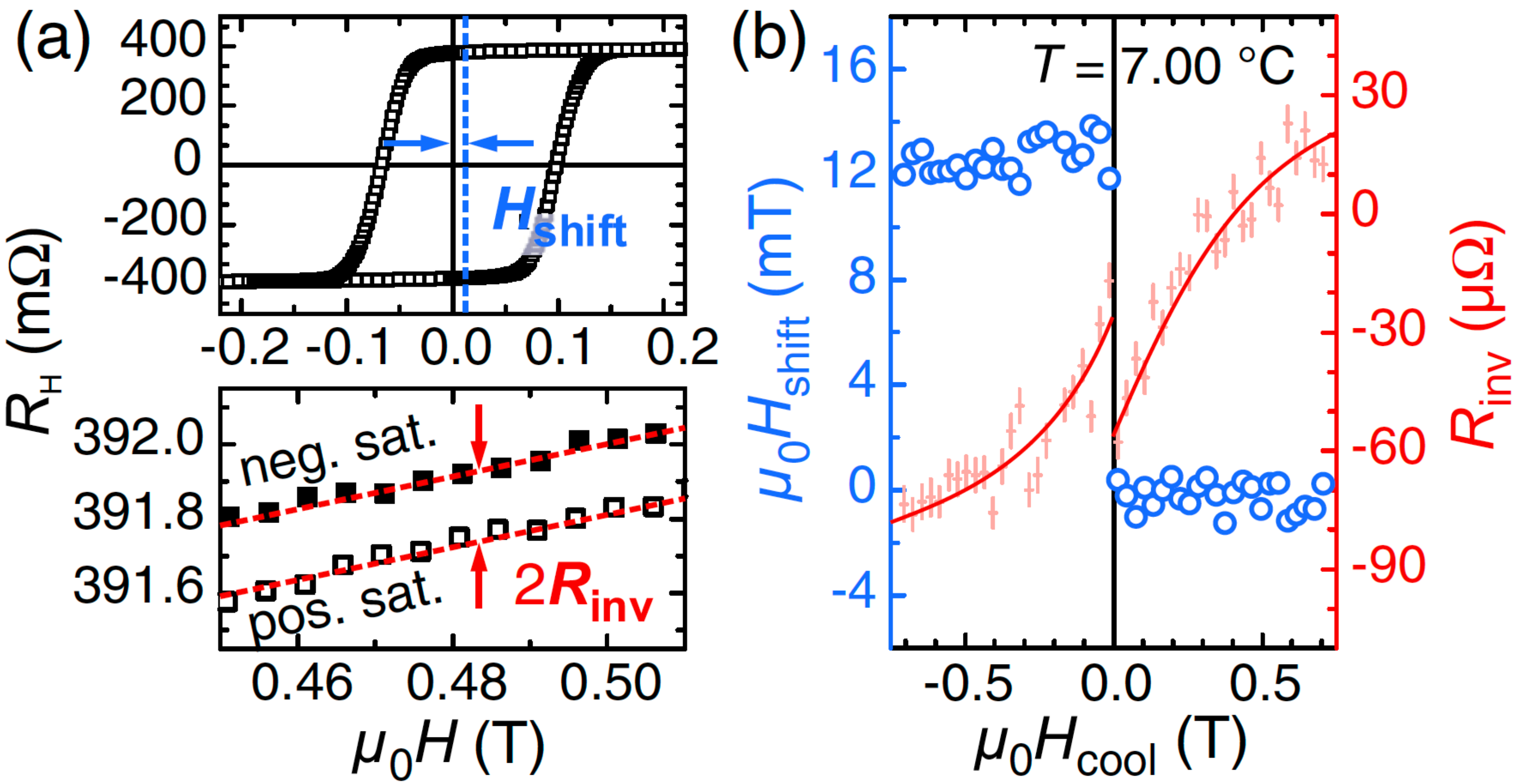

T. Kosub et al., *Phys. Rev. Lett.* **115**, 097201 (2015)

Heterostructures of ferro- and non-magnetic materials
Giant magnetoresistive effect

Anisotropic magnetoresistance (AMR): about 2% effect

AMR: electrical conductivity of ferromagnetic materials depends on the orientation of the magnetization with respect to the direction of the flowing current

Observed in 1856 by W. Thomson (Lord Kelvin)

W. Thomson,
Proc. Roy. Soc. (London) 8, 546 (1856/1857)

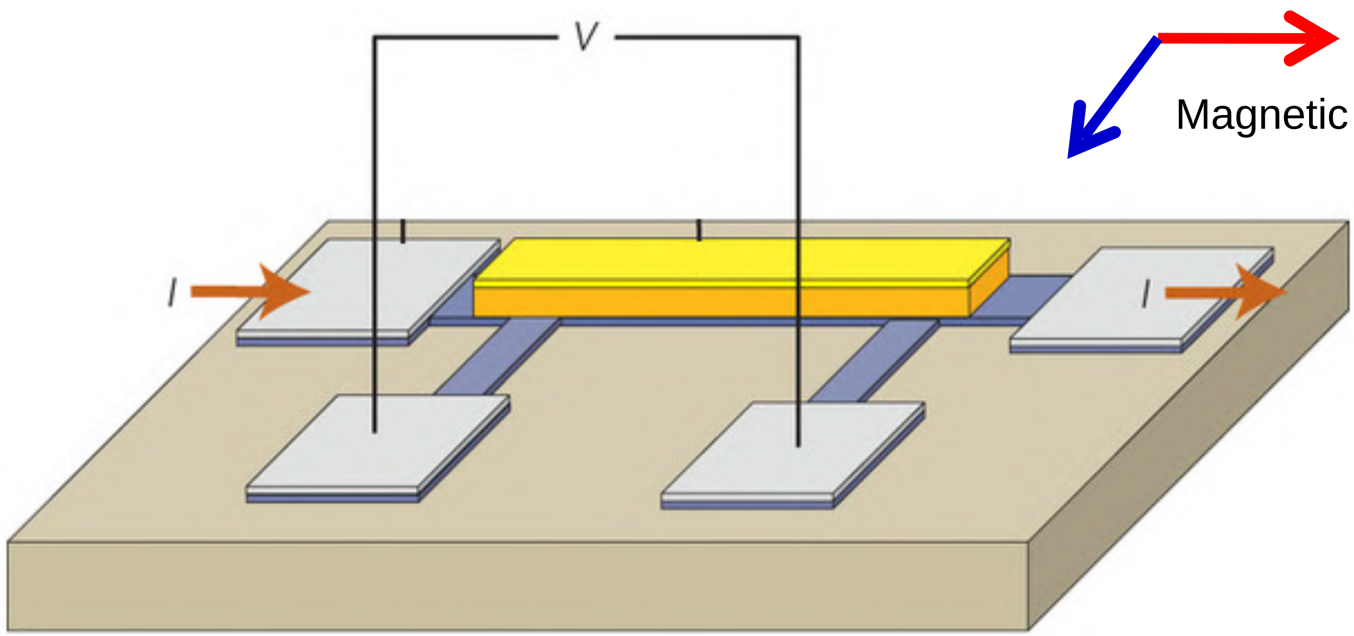

Explained by N.F. Mott in 1936: spin-orbit interaction needs to be accounted for

N.F. Mott, Proc. Roy. Soc. (London), Ser. A 153, 699 (1936).

Giant magnetoresistance (GMR): about 100% effect

GMR: change of the resistance of the magnetic multilayer stack in magnetic field

Application relevant for magnetic sensor devices

Typical GMR values: in the range of 20-100%

Current-in-plane (CIP) measurement scheme

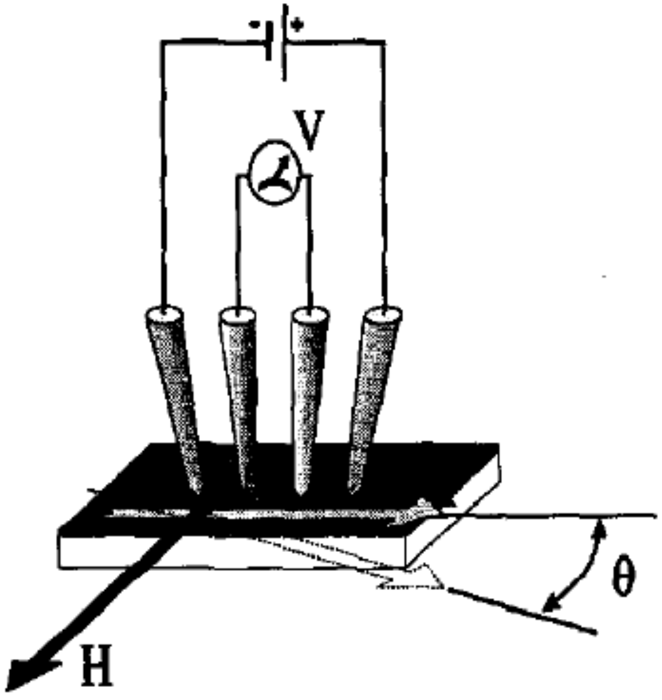

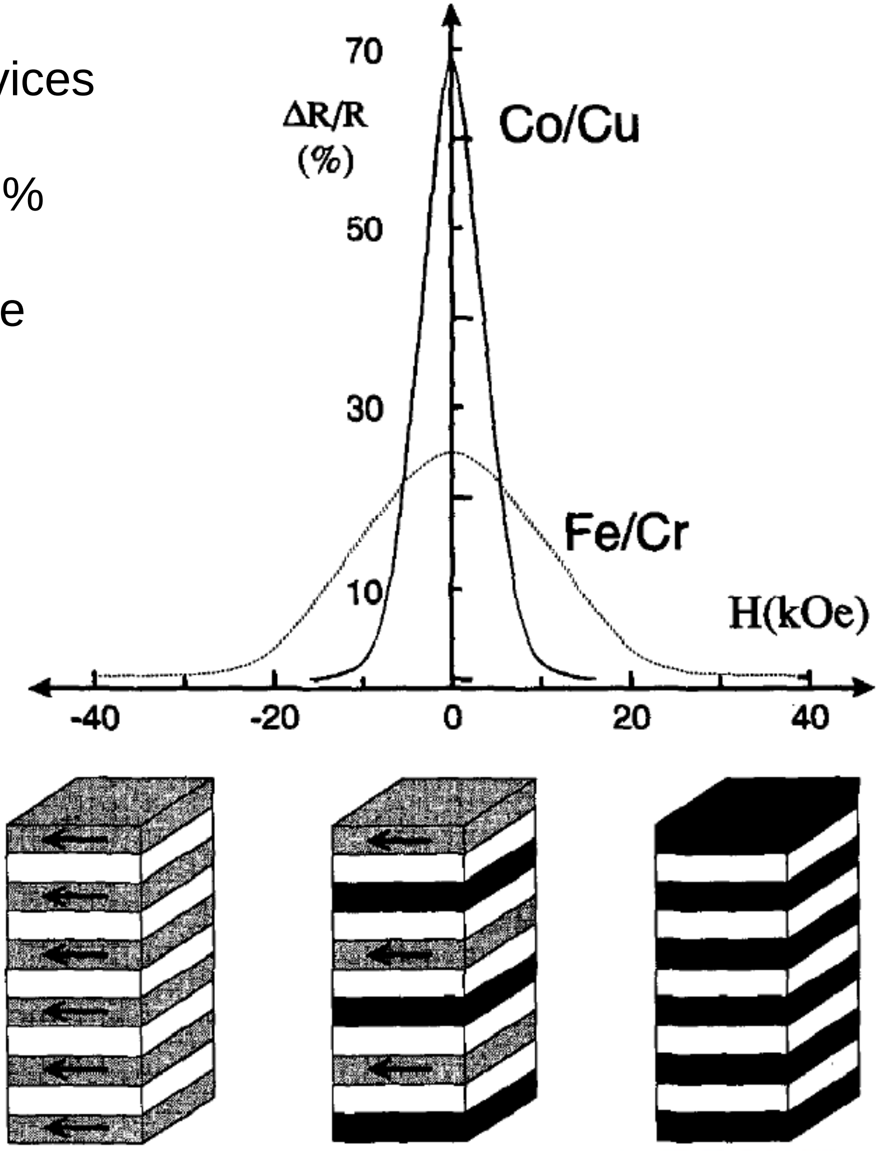

S.S.P. Parkin, *Annu. Rev. Mater. Sci.* **25**, 357 (1995)

Interlayer exchange coupling

Kerr microscopy image of the Fe/Cr bilayer with continuously varying Cr layer thickness

Lecture notes of the 40th IFF spring school: *Spintronics* (2009)

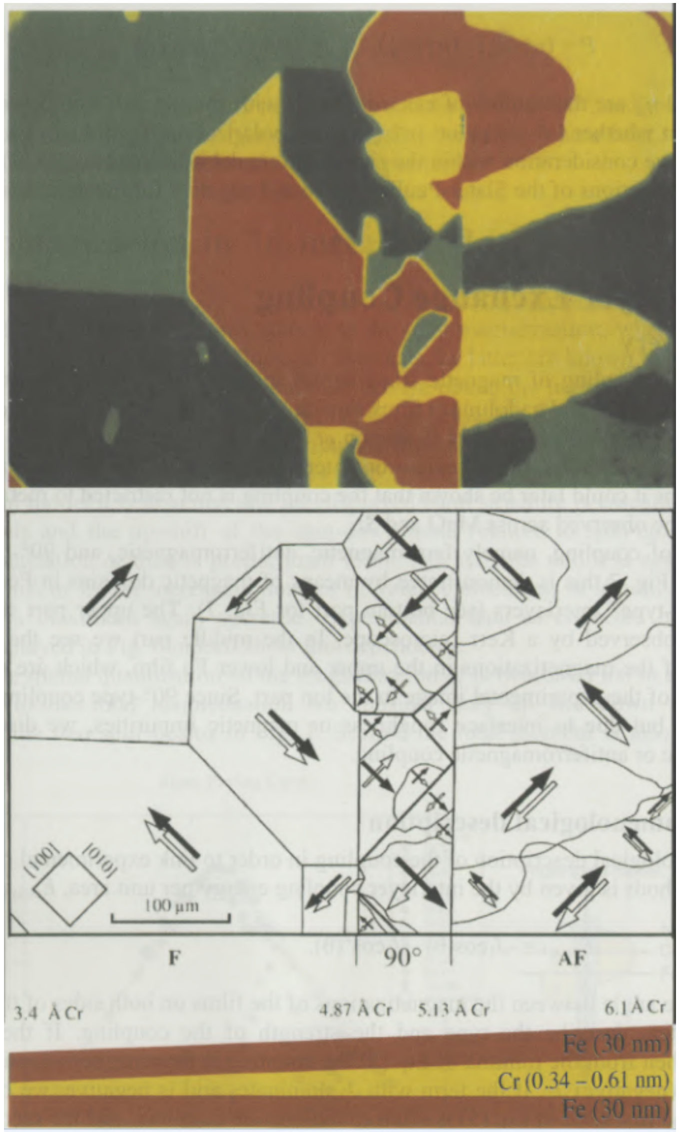

Dependent on the thickness of the spacer layer:

Ferromagnetic coupling

Antiferromagnetic coupling

90° coupling

Oscillating F-AF coupling dependent on the thickness of the spacer

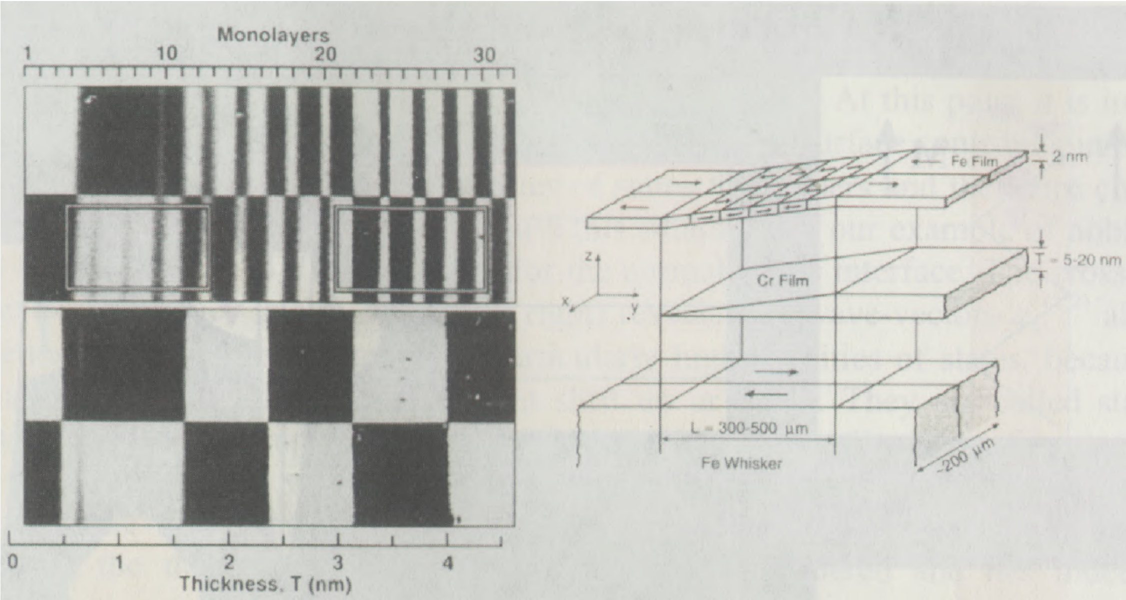

Dr. Denys Makarov I E-Mail: d.makarov@hzdr.de I Intelligent Materials and Systems

Tuning the sensitivity of the GMR sensor

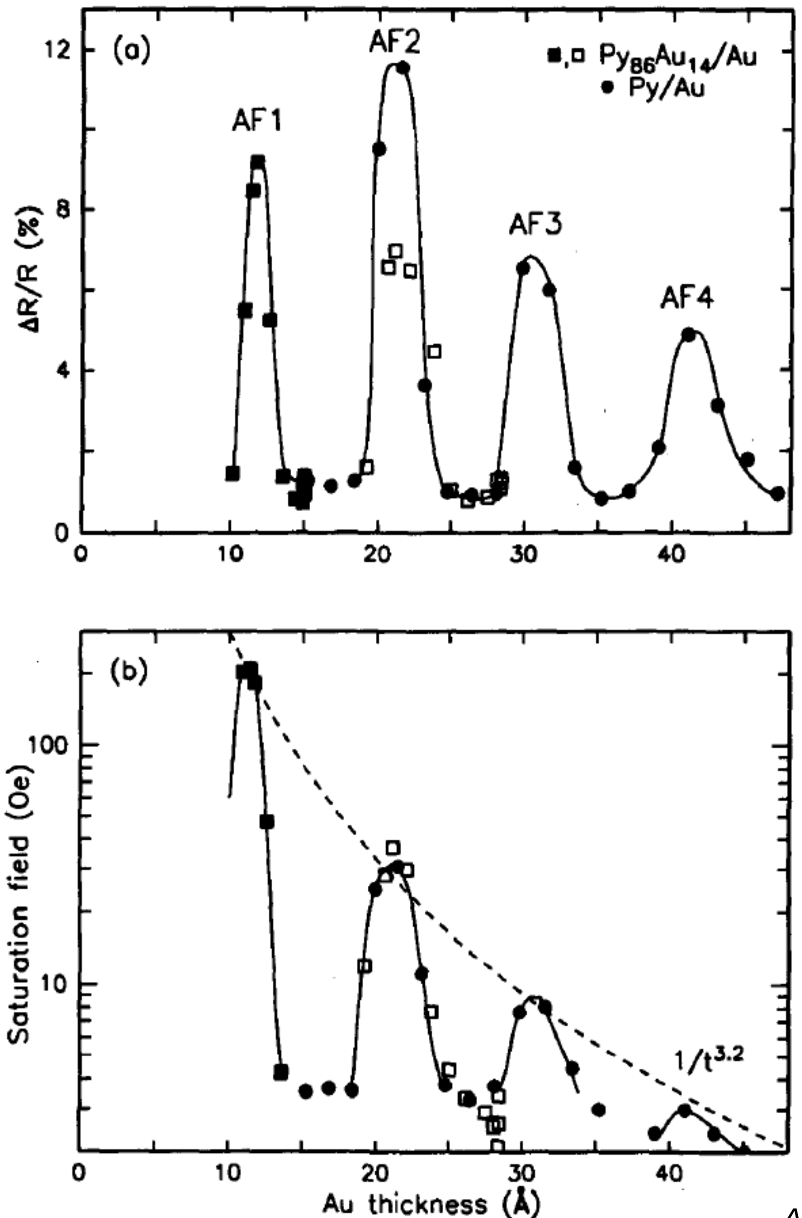

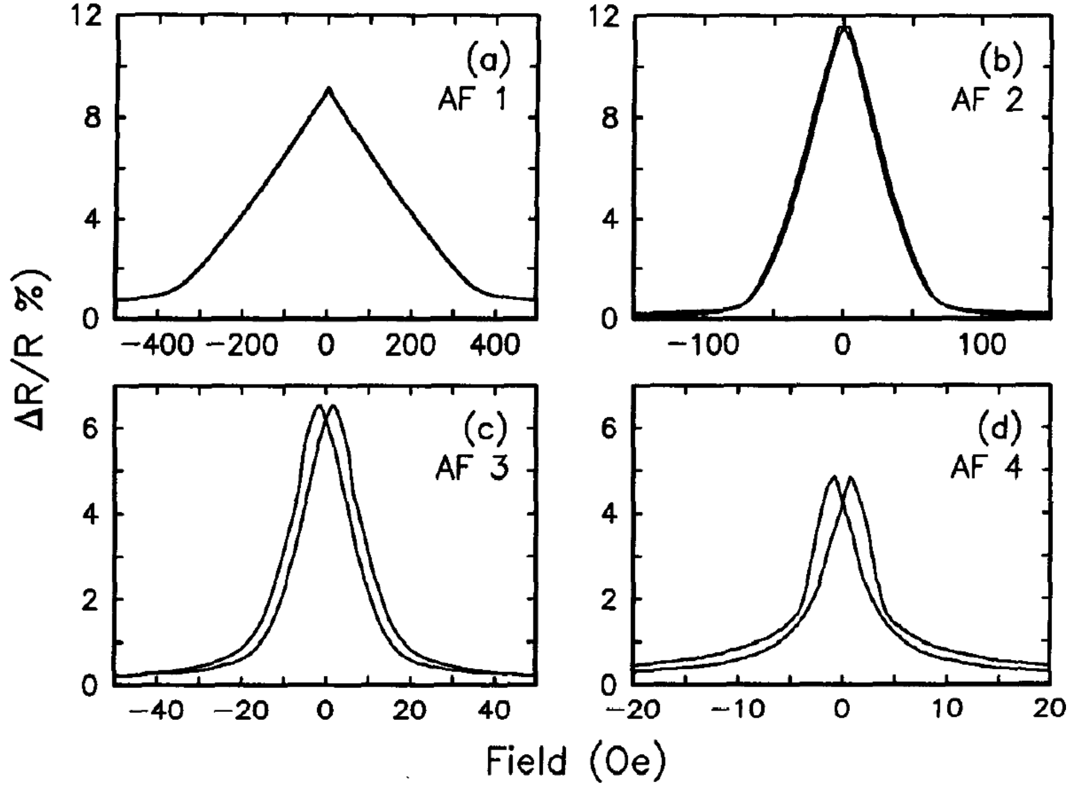

Different thickness of the Au spacer layer:

AF1: 11.7 Å (43 x10^{-6} Ohm cm)

AF2: 21.5 Å (19 x10^{-6} Ohm cm)

AF3: 29.8 Å (13 x10^{-6} Ohm cm)

AF4: 41.0 Å (10 x10^{-6} Ohm cm)

Annu. Rev. Mater. Sci. **25**, 357 (1995)

Microscopic origin of GMR

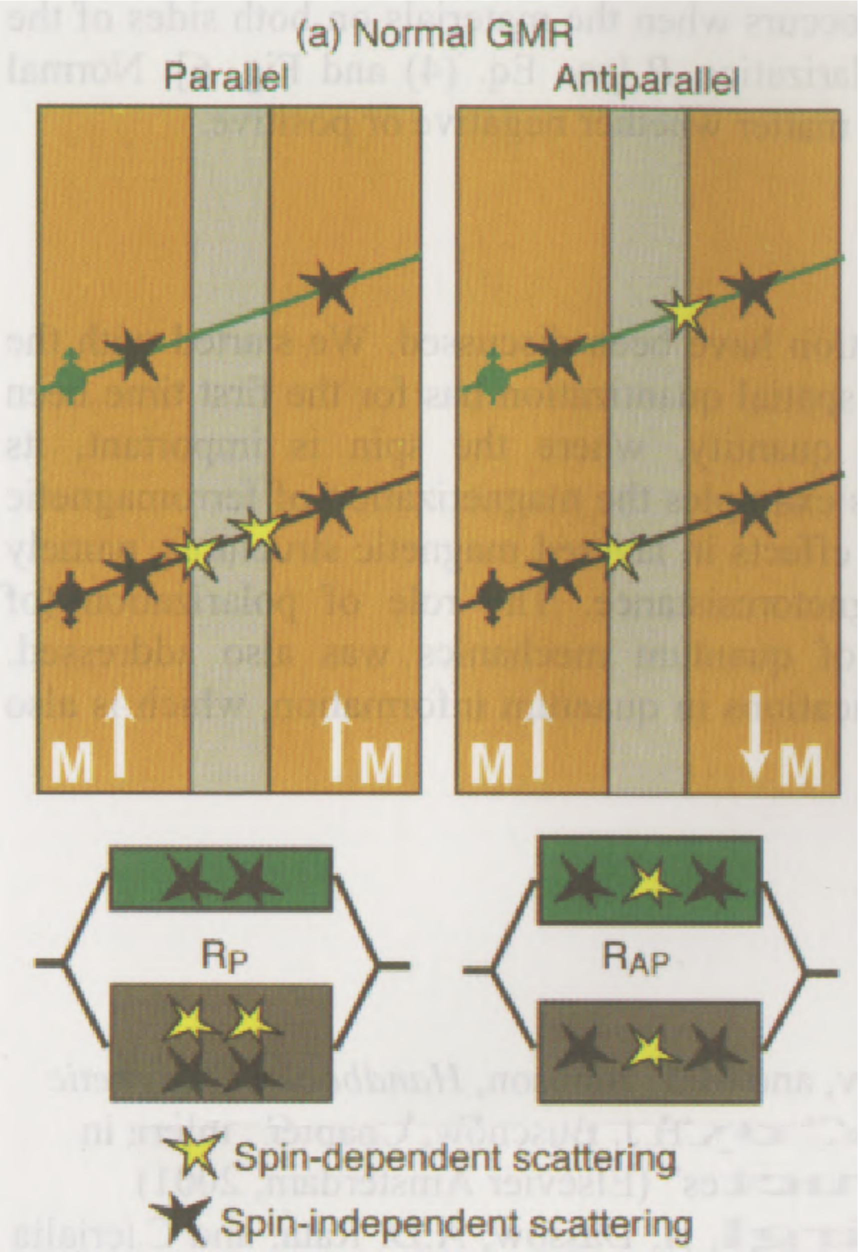

Following the two-current model by Mott

N.F. Mott, Proc. Roy. Soc. (London), Ser. A 153, 699 (1936)

Spin-dependent scattering at the interfaces

Scattering causes electrical resistance

Scattering inside the interlayer is neglected

Rates of spin-dependent and spin-independent scattering are the same

One scattering event contribute to the total resistance by an amount *r*

$$R_P = 2r \text{ x } 4r / (2r + 4r) = 8r/6$$

$$R_{AP} = 3r \text{ x } 3r / (3r + 3r) = 9r/6$$

$\Delta R/R_P$ = 12.5% (max in experiment = 17%)

Lecture notes of the 40th IFF spring school: *Spintronics* (2009)

Interlayer exchange coupling

Phenomenological description

Lecture notes of the 40th IFF spring school: *Spintronics* (2009)

Interlayer exchange coupling energy: $E_{coupl} = -J_1 \cos(\theta) - J_2 \cos^2(\theta)$

with θ – angle between the magnetizations of the films on both sides of the spacer layer

J_1 – bilinear coupling constant; J_2 – biquadratic coupling constant

Parameters J_1 and J_2 determines the strength and type of the coupling

If $J_1 >> J_2$ and J_1 is positive (negative) then the coupling will be ferromagnetic (antiferromagnetic)

If $J_2 >> J_1$ and is negative, 90° coupling is favorable

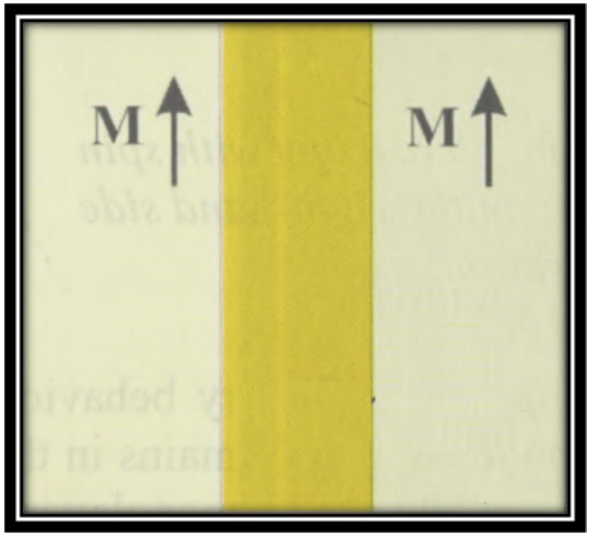

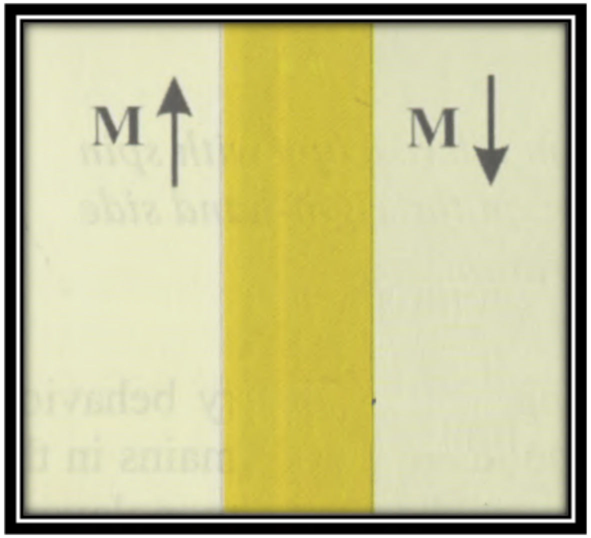

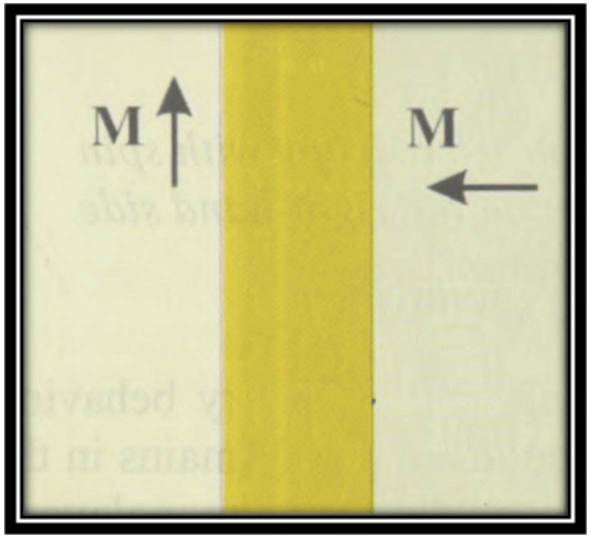

Heterostructures of ferro- and non-magnetic materials

Dzyaloshinskii–Moriya interaction

Physique **20**, 817 (2019)

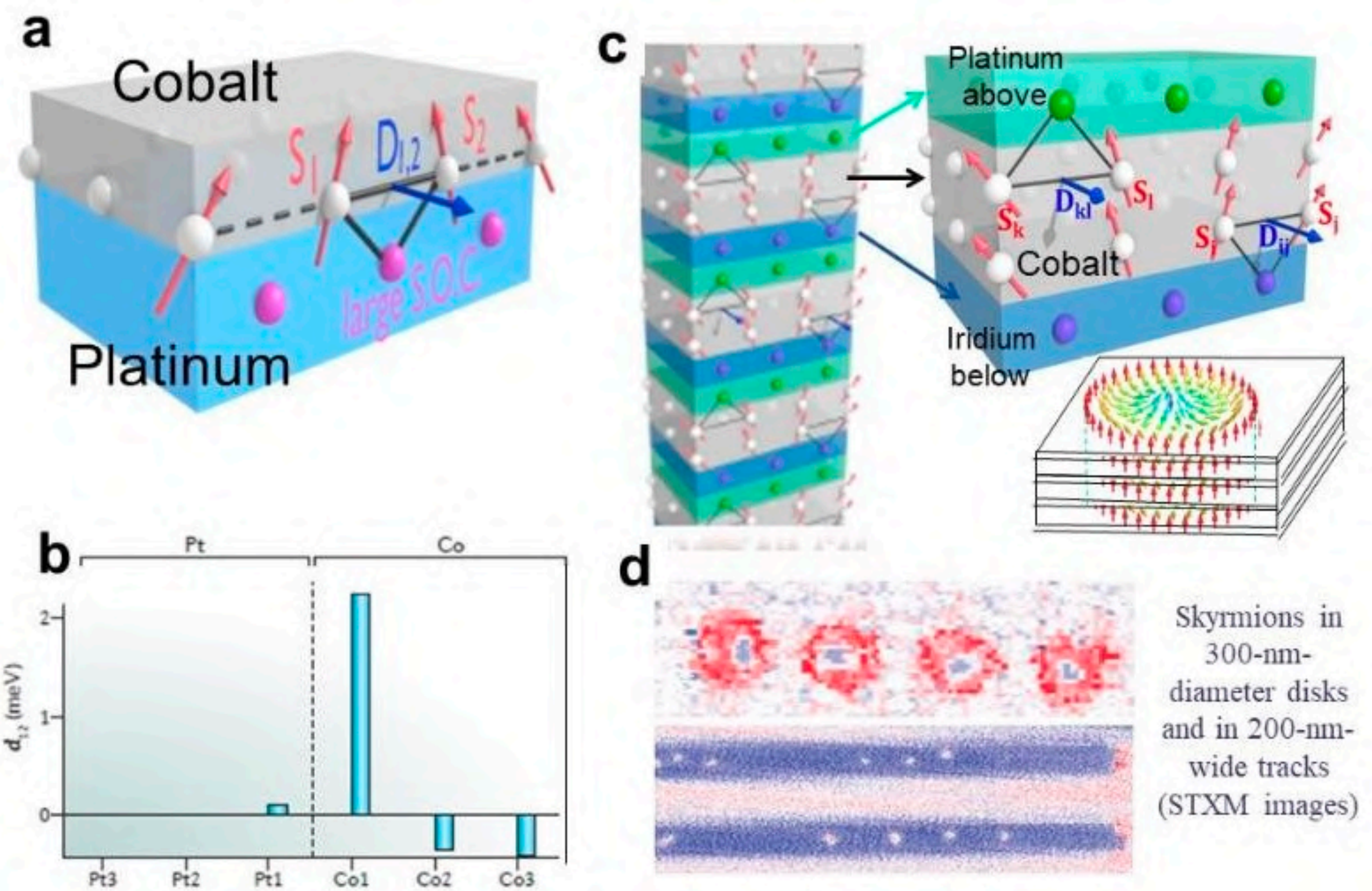

Skyrmions in 300-nm-diameter disks and in 200-nm-wide tracks (STXM images)

Heterostructures of ferro- and non-magnetic materials

Perpendicular magnetic anisotropy

AIP Advances **2**, 042182 (2012)

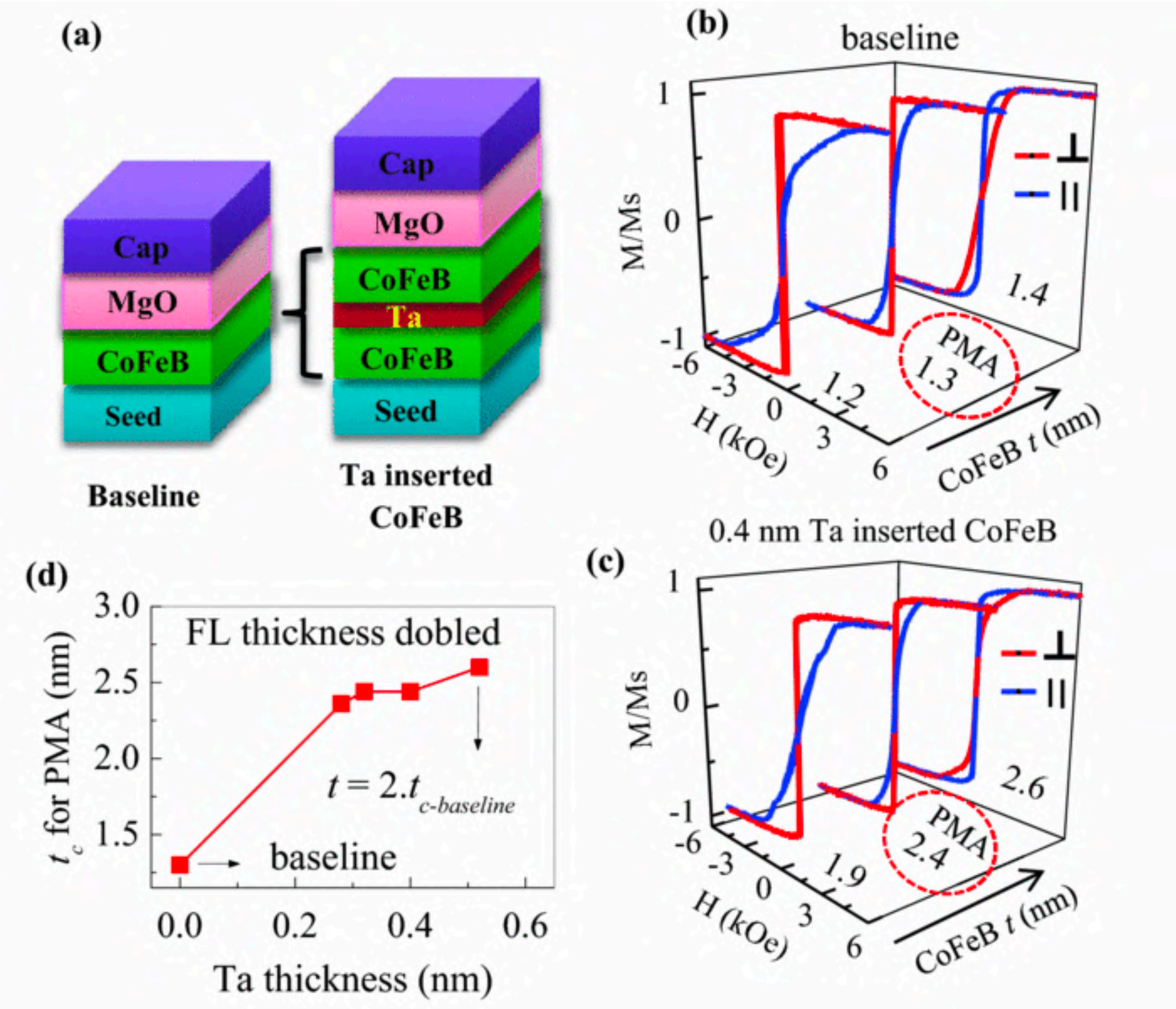

2D magnetic materials and heterostructures

2D magnetic materials and heterostructures

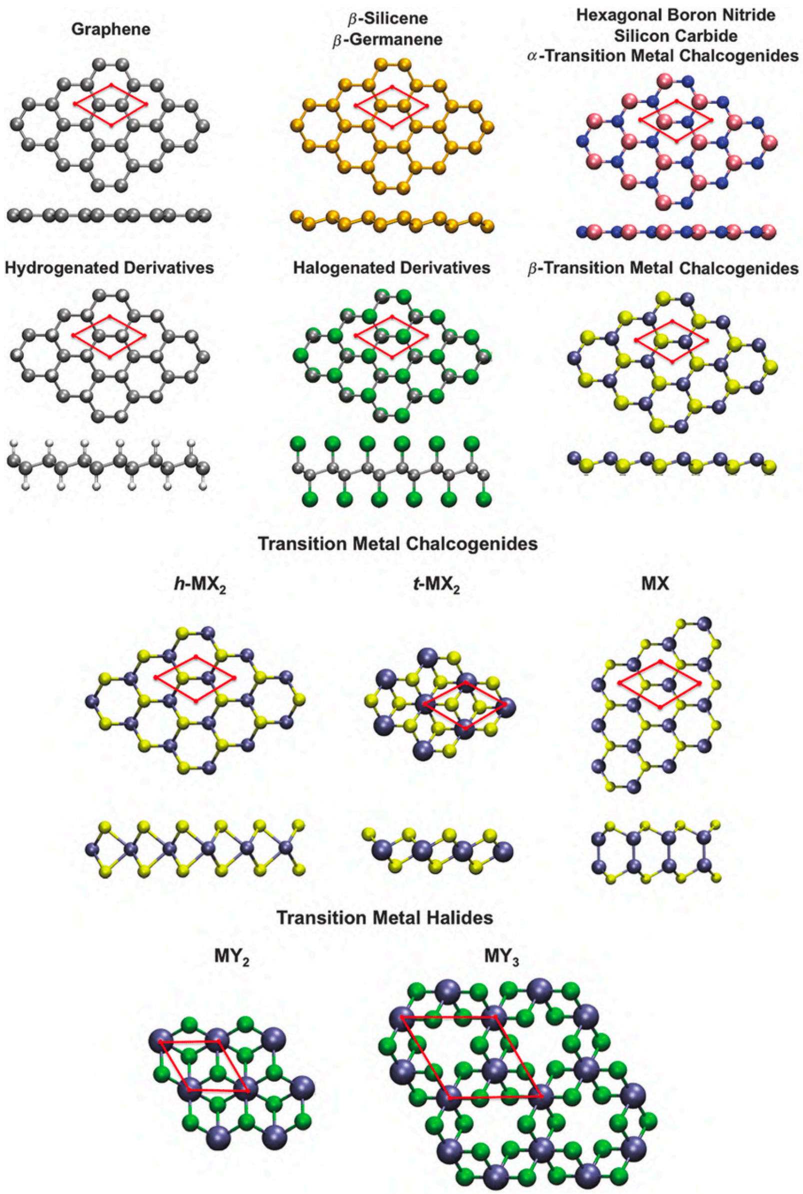

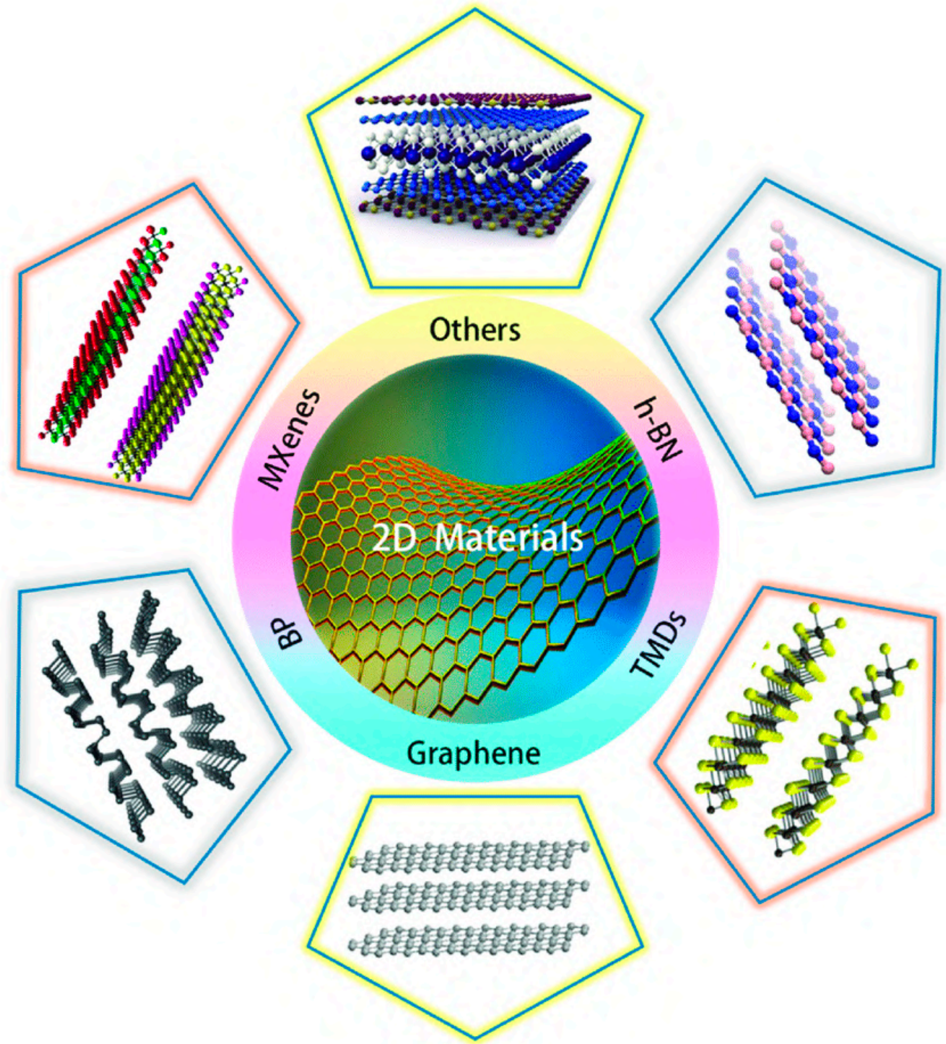

Molecules **24**, 88 (2019)

Chem. Soc. Rev. **43**, 6537 (2014)

Magnetic 2D materials and heterostructures

3D system: a magnetic phase transition occurs at a finite temperature

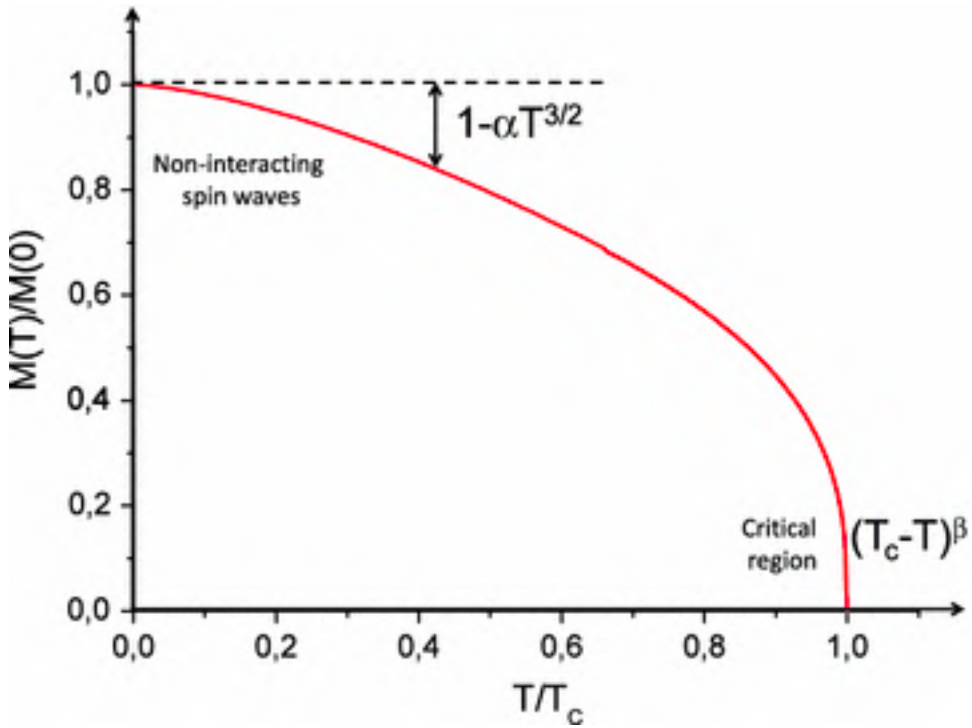

https://doi.org/10.1007/978-3-319-17897-4_17

Magnetic 2D materials and heterostructures

3D system: a magnetic phase transition occurs at a finite temperature

1D system: long-range order is possible only at $T = 0$ *Proc. Camb. Philos. Soc.* **32**, 477 (1936)

2D system: the existence of magnetic long-range order at any finite temperature crucially depends on the number *n* of relevant spin components, usually called spin dimensionality, and determined by the physical parameters of the system (for example, the presence and strength of magnetic anisotropy)

https://www.nature.com/articles/s41565-019-0438-6

Magnetic 2D materials and heterostructures

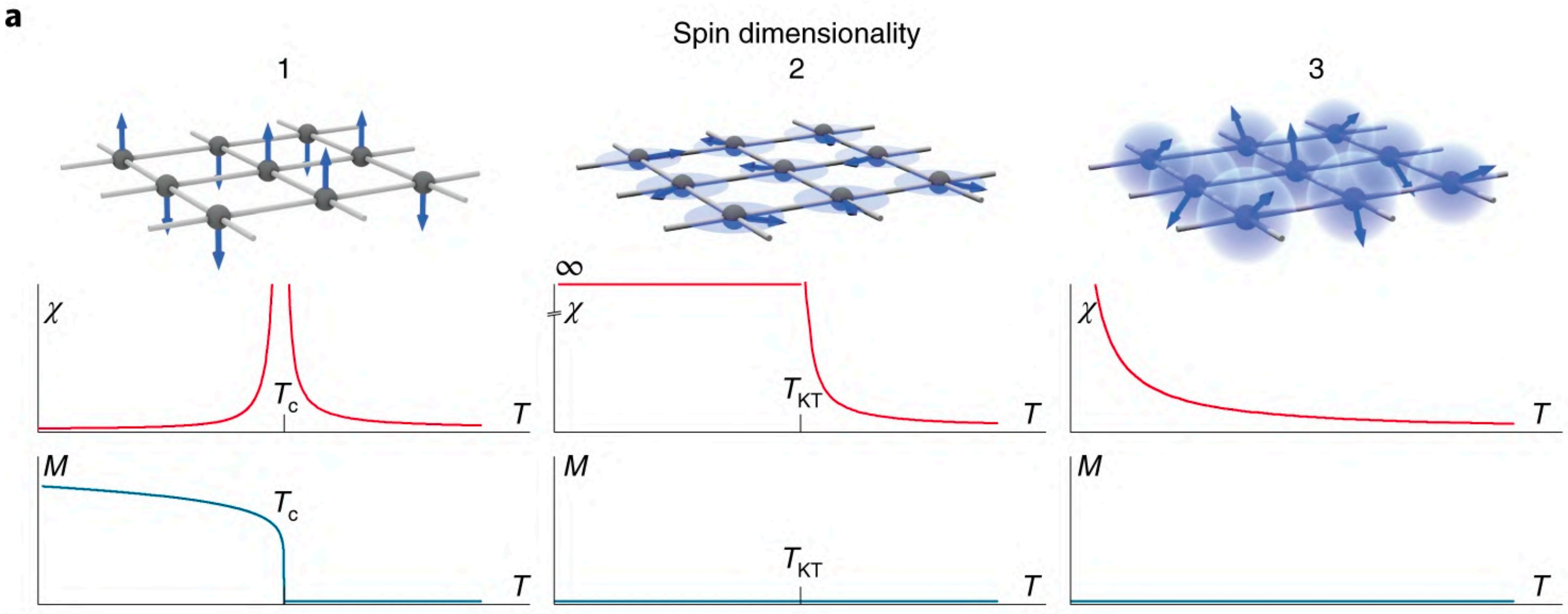

Spin dimensionality n = 1: the system has a strong uniaxial anisotropy and the spins point in either of the two possible orientations (‘up’ or ‘down’) along a given direction

Spin dimensionality n = 2 corresponds to an easy-plane anisotropy that favours the spins to lie in a given plane, although the orientation within the plane is completely unconstrained.

Isotropic systems are characterised with n = 3: there is no constraint on the direction of spins

https://www.nature.com/articles/s41565-019-0438-6

Mermin-Wagner(-Hohenberg) theorem

Phys. Rev. Lett. **17**, 1133 (1966)
Phys. Rev. **158**, 383 (1967)

Thermal fluctuations destroy long-range magnetic order in 2D systems at any finite temperature when the spin dimensionality is 3 (isotropic Heisenberg model)

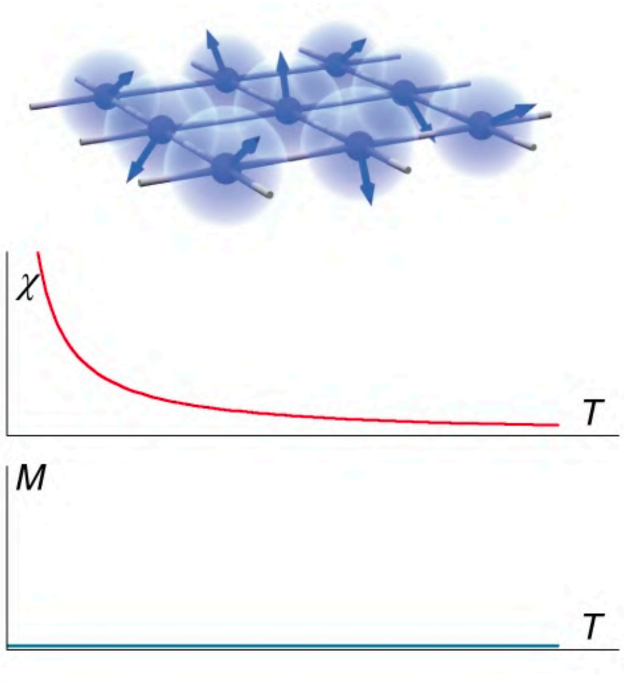

There is no isotropic 2D ferromagnet: long-wavelength excitations (spin waves) can be excited at any finite temperature as there is no gap in the spin wave spectrum (no anisotropy)

https://www.nature.com/articles/s41565-019-0438-6

2D magnet with n = 2

These systems are described by the so-called XY model

They do not possess a conventional transition to long-range order

The susceptibility diverges below a finite temperature

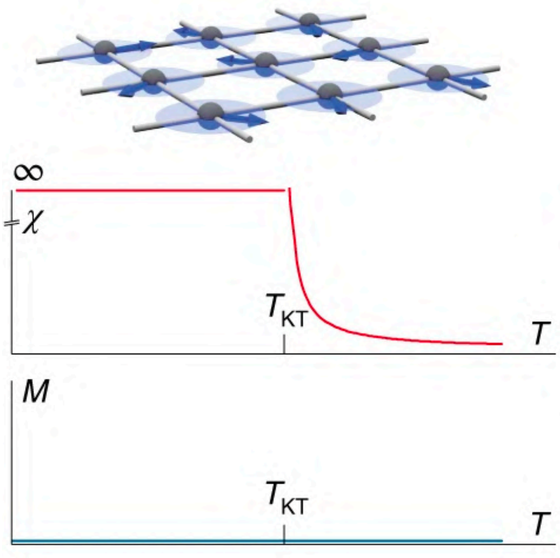

Berezinskii, Kosterlitz and Thouless pointed out that this divergence is associated with the onset of topological order, characterized by an algebraic decay of spin correlations and by the presence of bound pairs of vortex and antivortex arrangements of spins

Sov. Phys. JETP-USSR **32**, 493 (1971)
J. Phys. C. **6**, 1181 (1973)

Below the Kosterlitz–Thouless temperature T_{KT}, quasi-long-range magnetic order is established, and the existence of a finite order parameter is suppressed only marginally with the system size

https://www.nature.com/articles/s41565-019-0438-6

CrI3

- Semiconducting layered vdW material
- Undergoes low-temperature magnetic transitions
- Exhibits different forms of magnetic order

Magnetization and magnetic susceptibility measurements show that bulk CrI_3 is a strongly anisotropic ferromagnet below the Curie temperature (T_c = 61 K), with its easy axis pointing perpendicular to the layers, and a saturation magnetization consistent with a spin S = 3/2 state of the Cr atoms

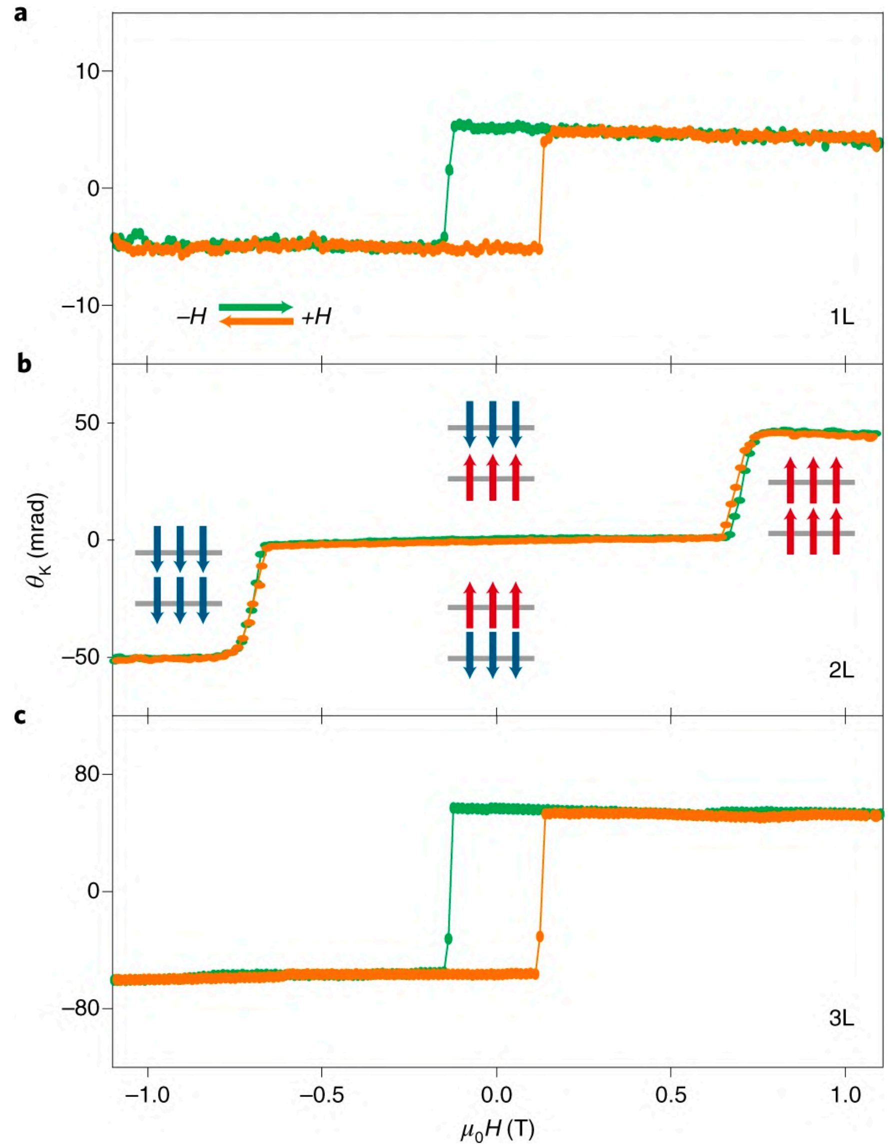

Nature **546**, 270–273 (2017)

https://www.nature.com/articles/s41565-019-0438-6

Dr. Denys Makarov I E-Mail: d.makarov@hzdr.de I Intelligent Materials and Systems

Magnetic 2D materials and heterostructures

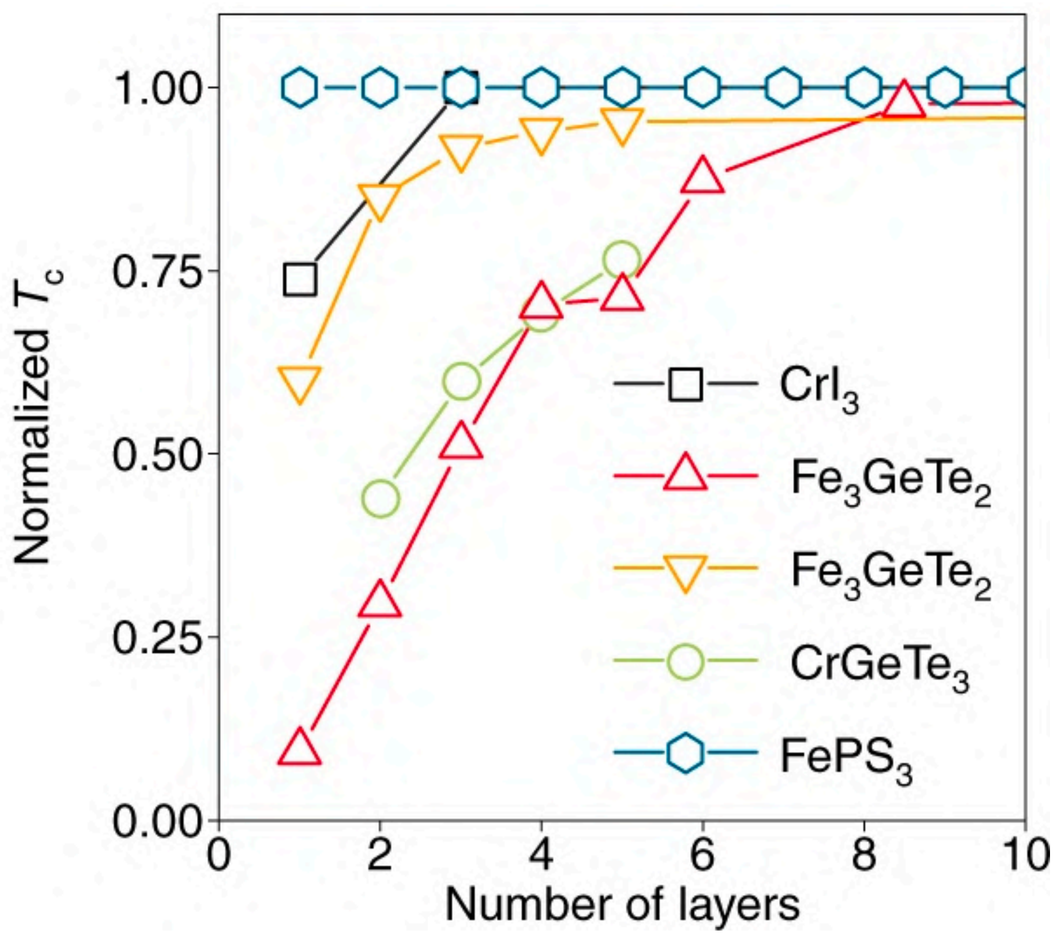

https://www.nature.com/articles/s41565-019-0438-6

Dr. Denys Makarov I E-Mail: d.makarov@hzdr.de I Intelligent Materials and Systems

Heterostructures with semiconducting TMDCs

Heterostructure of a ferromagnetic semiconductor CrI_3 and a monolayer of WSe_2

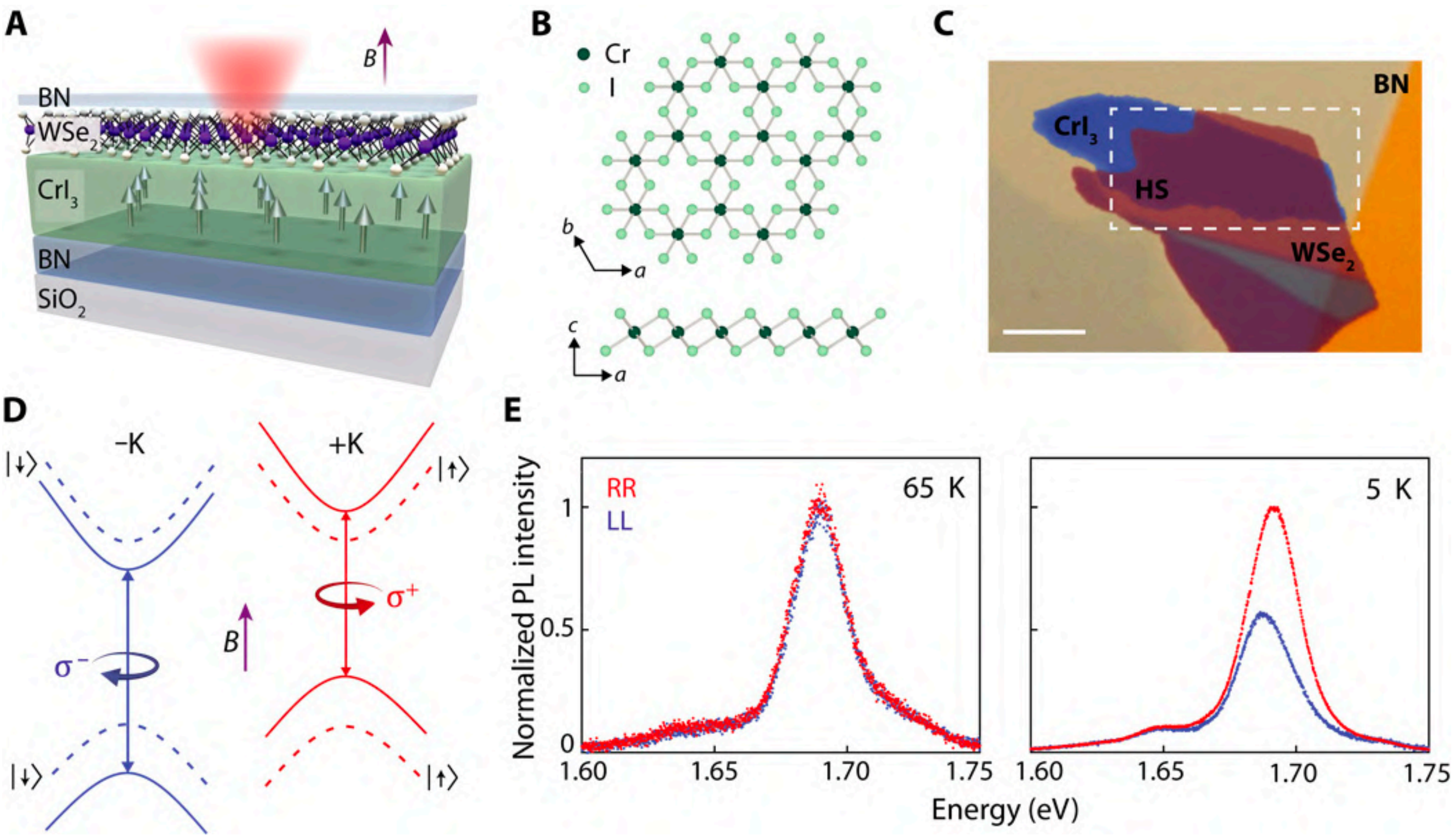

Sci. Adv. **3**, e1603113 (2017)

2D materials based magnetic tunnel junctions

Fe_3GeTe_2 / hBN / Fe_3GeTe_2 stack

Metallic 2D ferromagnet: Fe_3GeTe_2

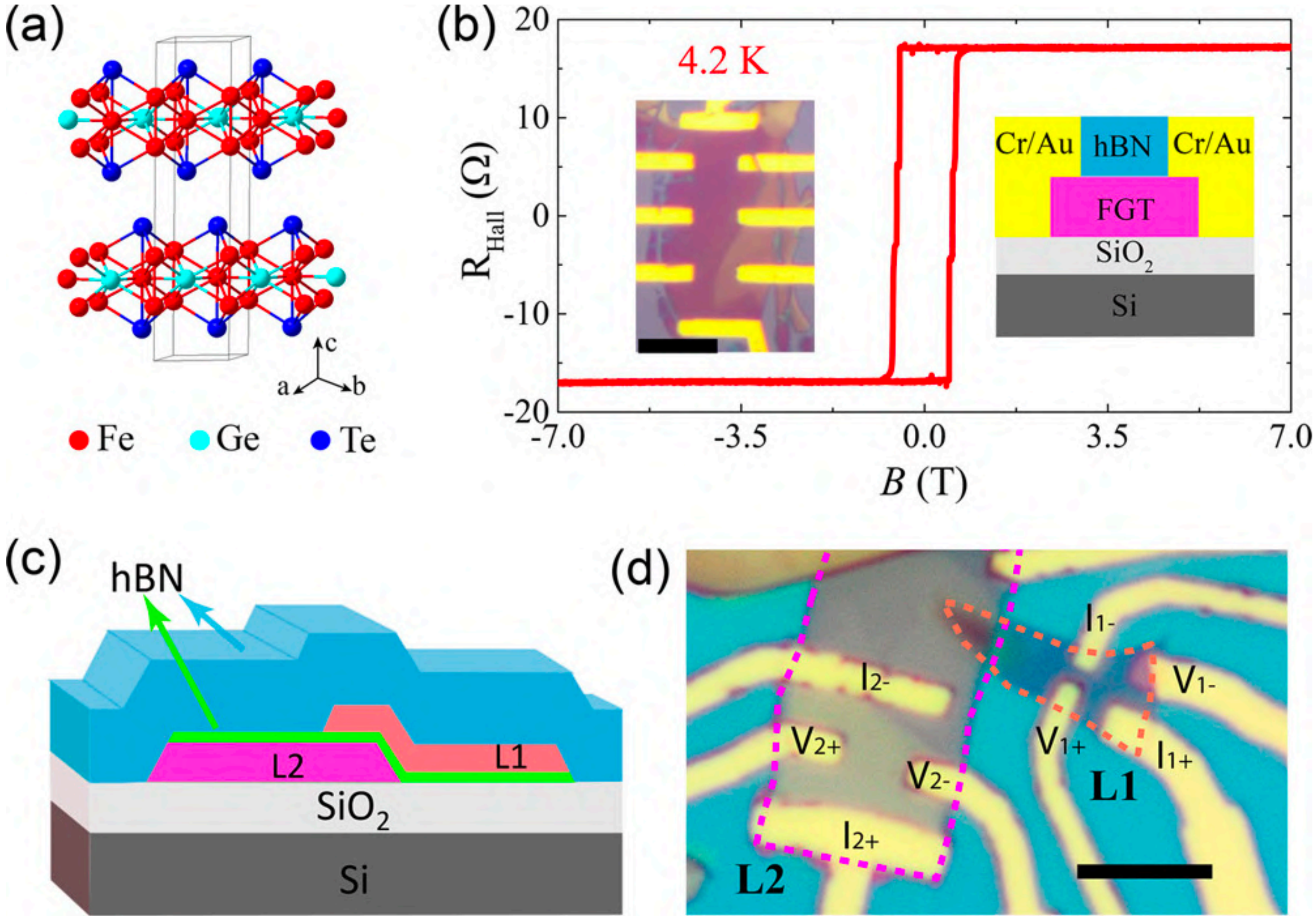

Nano Lett. **18**, 4303 (2018)

2D materials based magnetic tunnel junctions

Fe_3GeTe_2 / hBN / Fe_3GeTe_2 stack

Metallic 2D ferromagnet: Fe_3GeTe_2

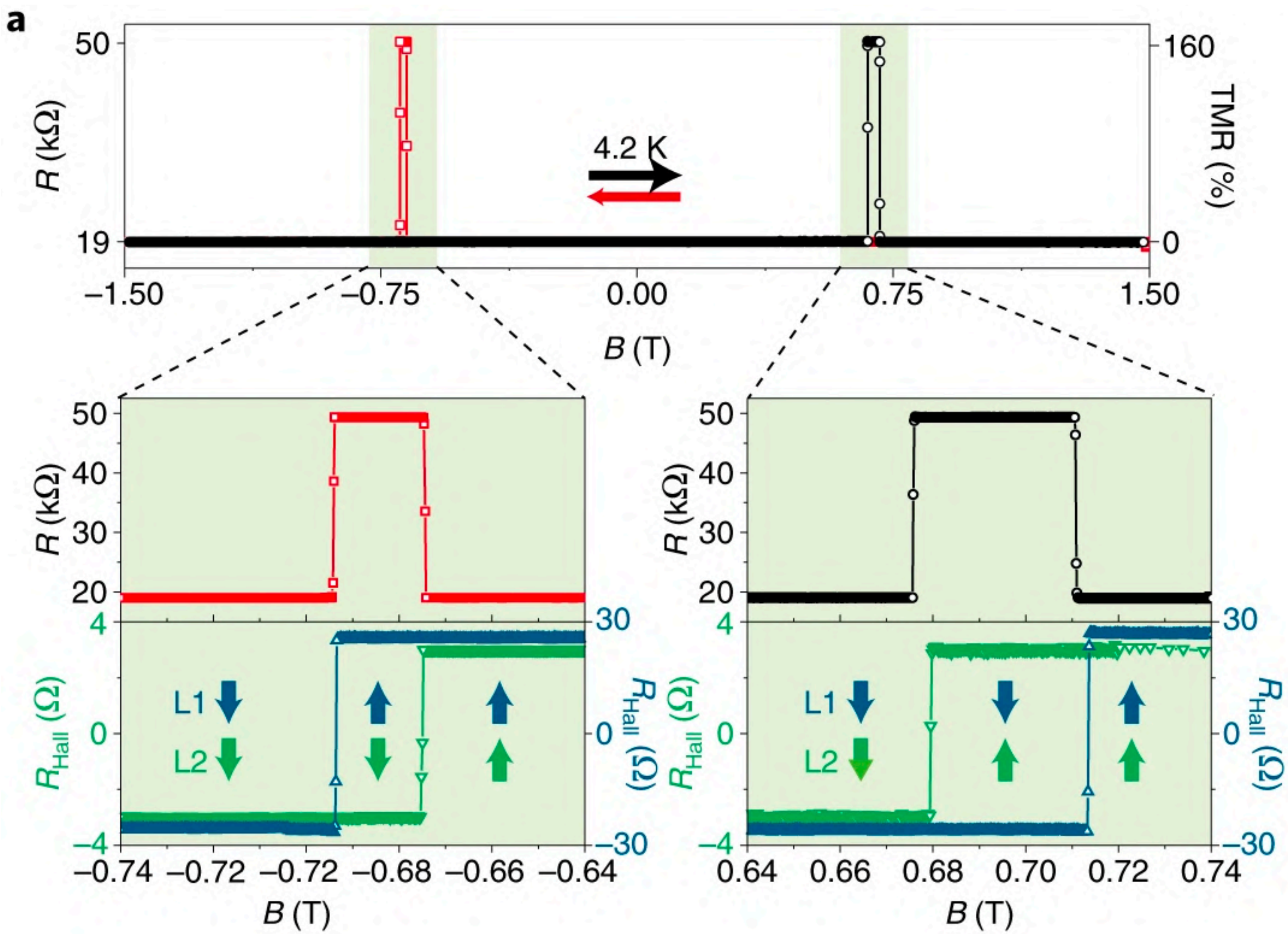

Nano Lett. **18**, 4303 (2018)

2D materials based magnetic tunnel junctions

Fe_3GeTe_2 / hBN / Fe_3GeTe_2 stack

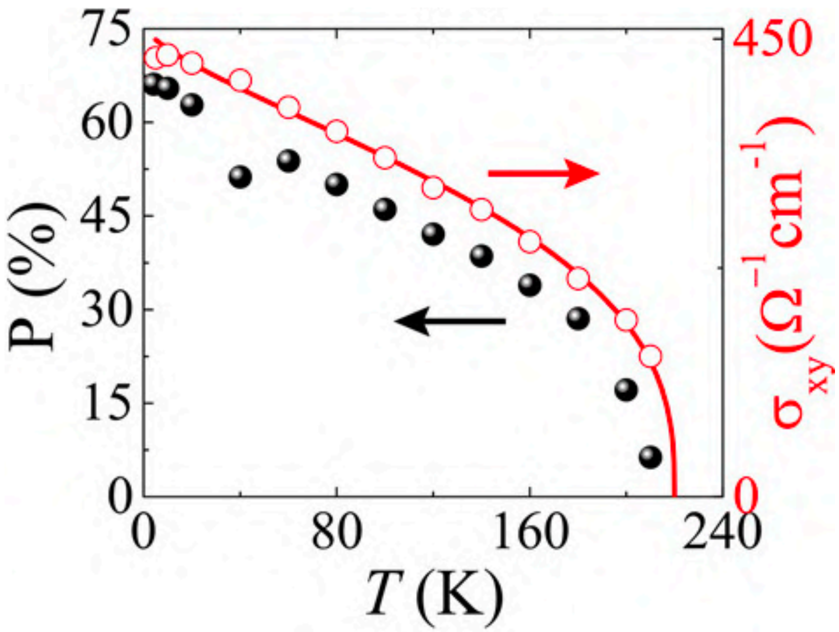

Metallic 2D ferromagnet: Fe_3GeTe_2

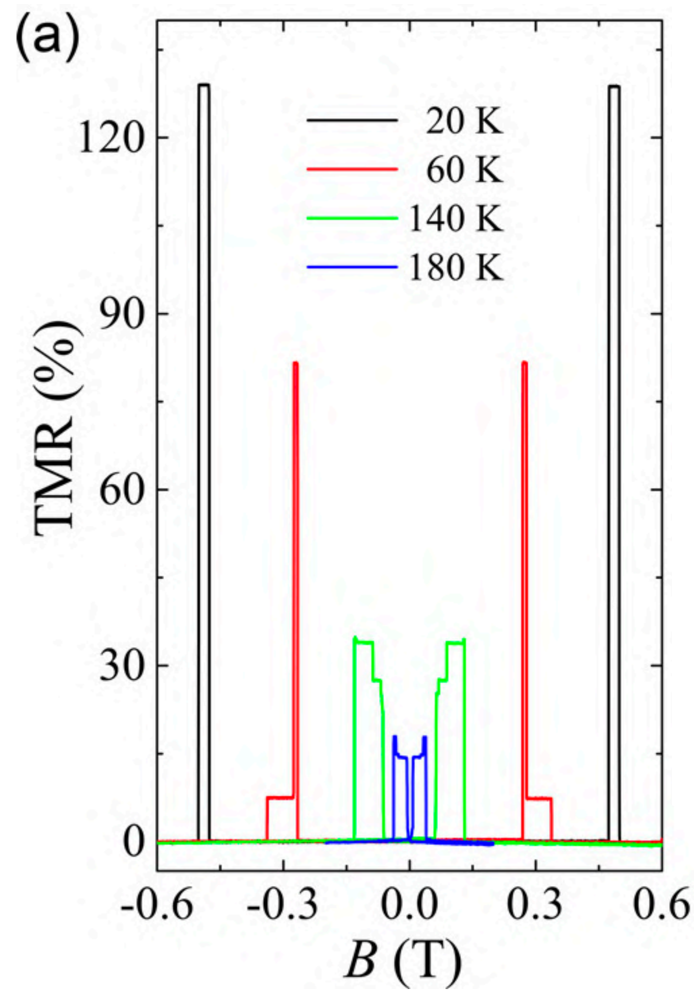

Nano Lett. **18**, 4303 (2018)

Magnetic Material – Topological Insulator Heterostructures

Dr. Denys Makarov I E-Mail: d.makarov@hzdr.de I Intelligent Materials and Systems

Magnetic topological insulators

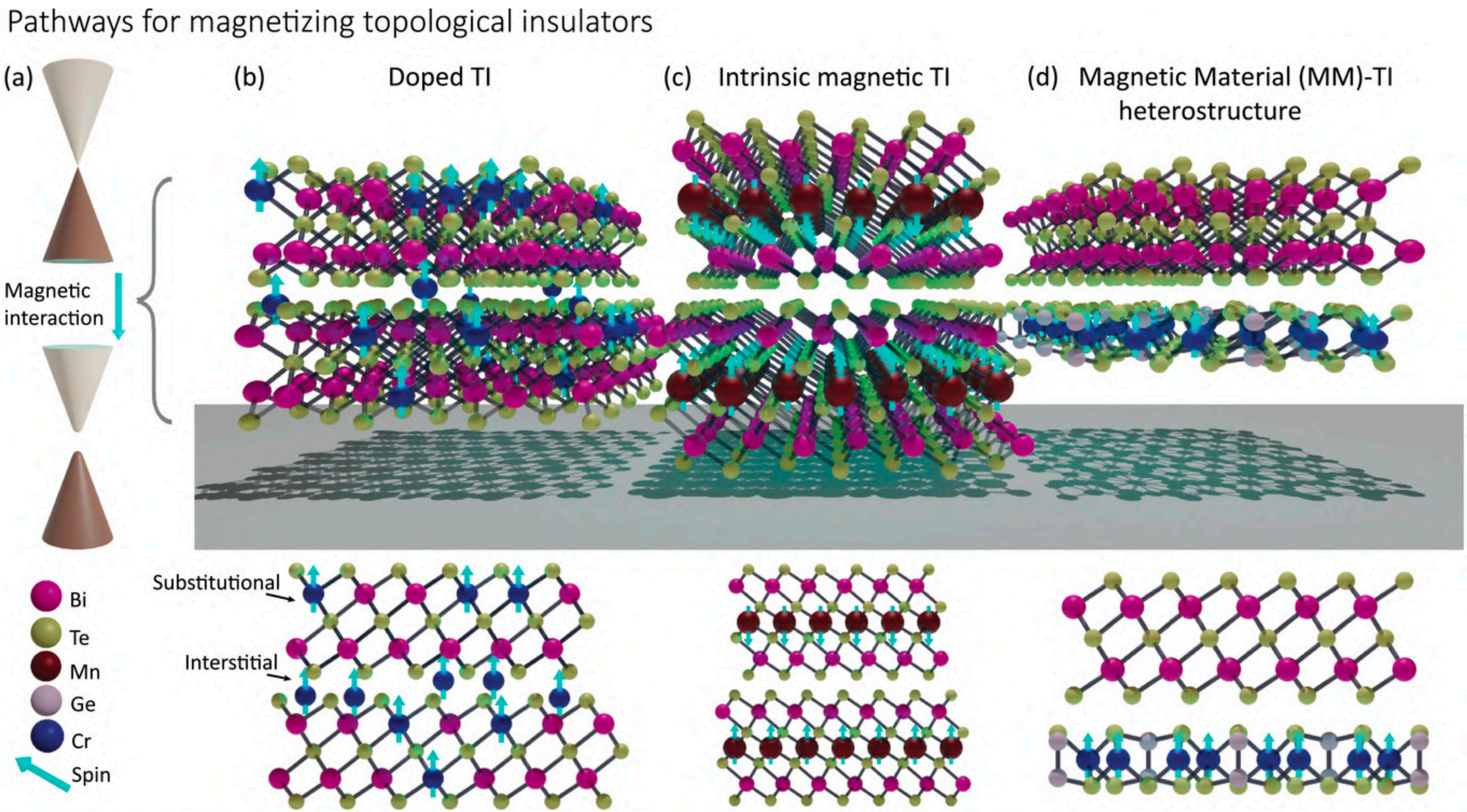

$(Cr_x,Bi_{1-x})_2Te_3$ $MnBi_2Te_4$ Bi_2Te_3–$Cr_2Ge_2Te_6$

https://onlinelibrary.wiley.com/doi/full/10.1002/adma.202007795

Heterostructure: ferromagnet and topological insulator

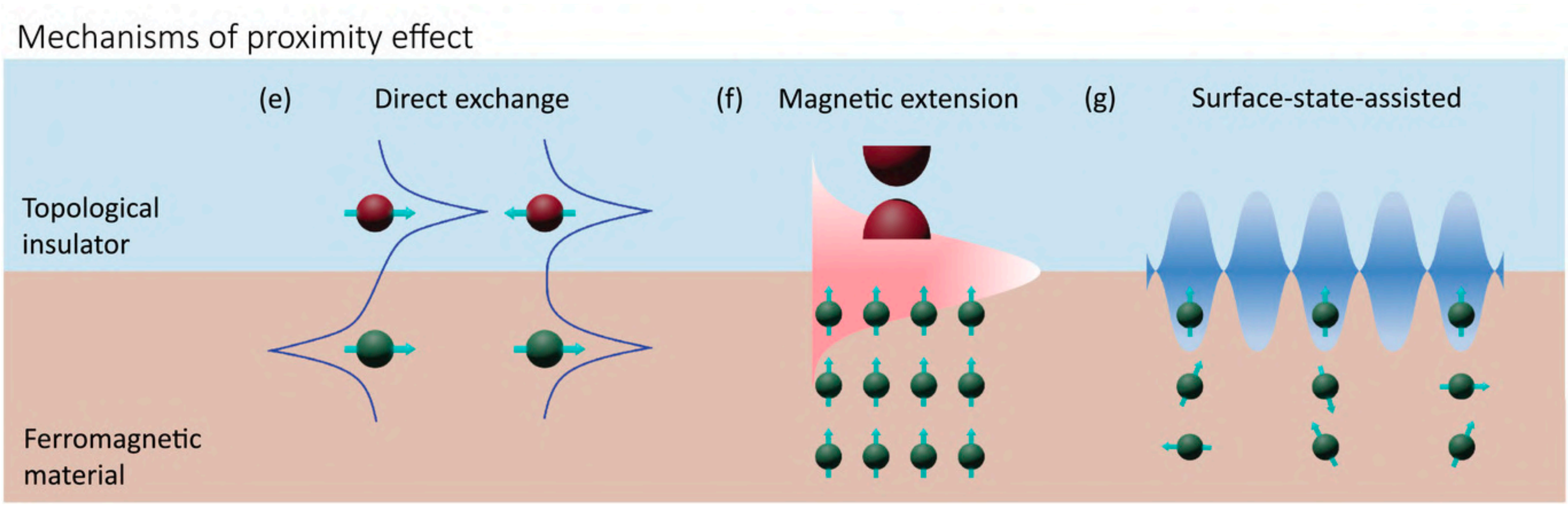

Magnetic proximity effect has a relatively short length scale (few Å). Hence, time-reversal symmetry is broken only at the interface of the TI and MM, and not in the bulk of the TI.

Therefore, typically TI must be sandwiched in between two layers of magnetic insulator (MI) with perpendicular magnetic anisotropy

Sci. Adv. **5**, eaaw1874 (2019)

https://onlinelibrary.wiley.com/doi/full/10.1002/adma.202007795

Anomalous Hall effect in FM/TI heterostructures

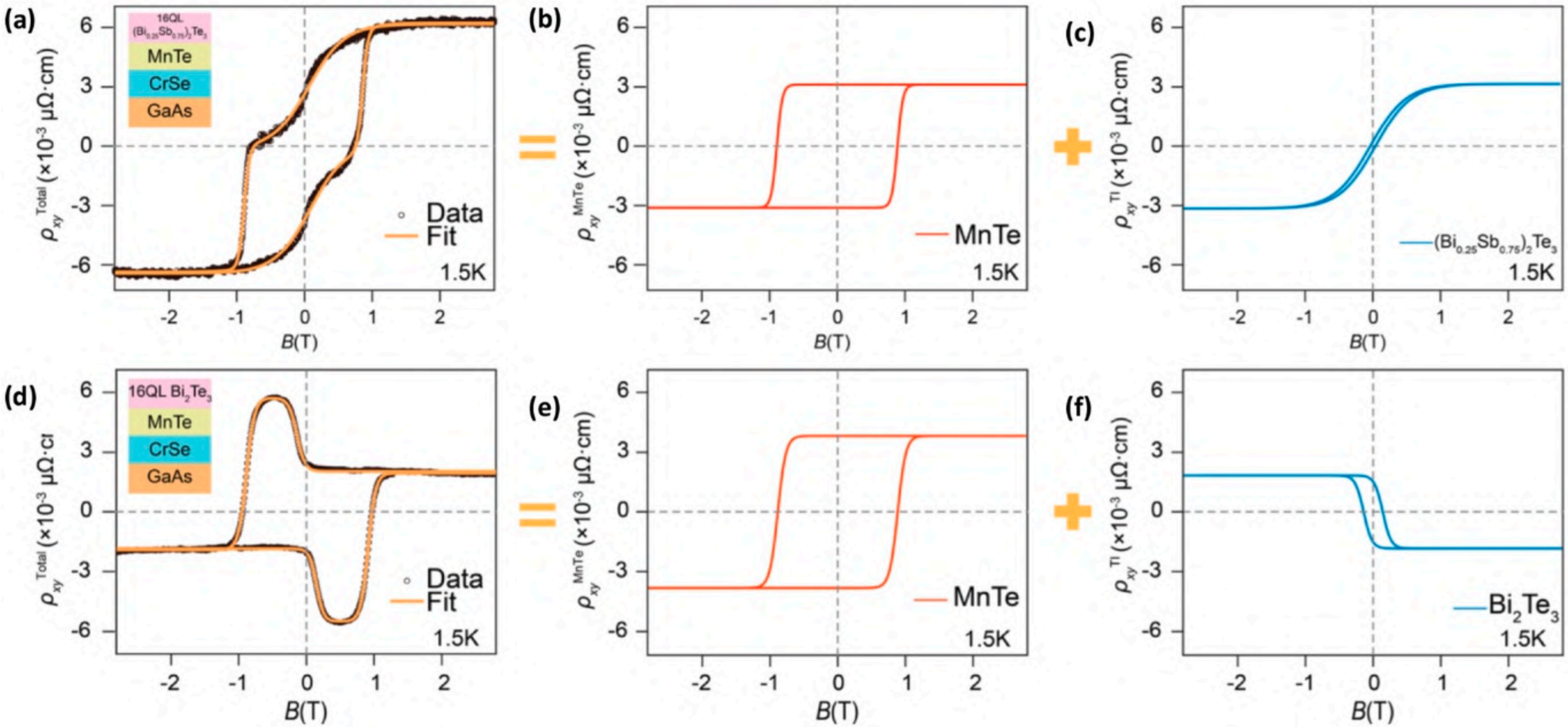

a) p-type 16 quintuple layer (QL) $(Bi_{0.25}Sb_{0.75})_2Te_3$–MnTe heterostructure and d) n-type 16 QL Bi_2Te_3–MnTe heterostructure

Nano Lett. **20**, 1731 (2020)

[magnetic material] / TI heterostructures

Magnetic metal - TI heterostructure						
[118]	AFMM	CrSb	$Cr_x(Bi_{1-y}Sb_y)_{2-x}Te_3$	–	35 K	Neutron reflectometry, magnetometry, magneto-transport
[121]	AFMM	CrSb	$(Bi_{1-y}Sb_y)_2Te_3$	–	90 K	Magneto-transport
[206]	AFMM	CrSe	$(Bi_{1-y}Sb_y)_2Te_3$	–	120 K	Magneto-transport, Magnetometry, Neutron reflectometry

…and many more…

Magnetic metal - TI heterostructure						
[118]	AFMM	CrSb	$Cr_x(Bi_{1-y}Sb_y)_{2-x}Te_3$	–	35 K	Neutron reflectometry, magnetometry, magneto-transport
[121]	AFMM	CrSb	$(Bi_{1-y}Sb_y)_2Te_3$	–	90 K	Magneto-transport
[206]	AFMM	CrSe	$(Bi_{1-y}Sb_y)_2Te_3$	–	120 K	Magneto-transport, Magnetometry, Neutron reflectometry

…and many more…

Magnetic metal - TI heterostructure						
[118]	AFMM	CrSb	$Cr_x(Bi_{1-y}Sb_y)_{2-x}Te_3$	–	35 K	Neutron reflectometry, magnetometry, magneto-transport
[121]	AFMM	CrSb	$(Bi_{1-y}Sb_y)_2Te_3$	–	90 K	Magneto-transport
[206]	AFMM	CrSe	$(Bi_{1-y}Sb_y)_2Te_3$	–	120 K	Magneto-transport, Magnetometry, Neutron reflectometry

…and many more…

https://onlinelibrary.wiley.com/doi/full/10.1002/adma.202007795

Thank you for your attention

Dr. Denys Makarov I E-Mail: d.makarov@hzdr.de I Intelligent Materials and Systems